(BL8A)

Fourier-Transform Spectroscopy and Photon Echo in Vacuum Ultraviolet Region

S. Asaka[A] and H. Nakatsuka[B]

[A]*Equipment Development Center, Institute for Molecular Science, Okazaki 444-8585*
[B]*Institute of Applied Physics, University of Tsukuba, Tsukuba 305-0004*

We have performed accumulated photon echo experiments by using synchrotron radiation (SR) in near vacuum ultraviolet region.

Photon echo experiments generally give us information of optical T_2, or the phase relaxation time of the sample resonance lines. Among many types of photon echoes, the accumulated photon echo has excellent features in that it gives a signal magnitude and a signal-to-noise ratio much larger than other types of photon echoes by using repetitively pulsed or quasi continuous excitation source. Furthermore, the time resolution in measuring T_2 is simply determined by the correlation time (i.e. the inverse of spectral width) of the source so that a femtosecond resolution can be easily achieved by using a wide-spectral-band source.

A periodic but static change of light intensity is formed over spectral axis if time-delayed two light beams are present. This structure is copied into the inhomogeneously broadened resonance line of the sample, thus forming a "population grating". The accumulated photon echo is based on the diffraction of the excitation light by this population grating. If the electrons of the sample stay a long time at some bottleneck state other than the ground state after resonant transition, the population grating in the ground state accumulates over the bottleneck lifetime, resulting in a large echo signal.

The SR is useful as an excitation source for accumulated photon echo experiments because it is quasi continuous and it has a wide spectral band especially in short wavelength region, where other light sources cannot give sufficient light intensity for echo measurements. The echo time resolution is, for example, 40 fs if we cut out a spectral portion of SR by a width of 0.1 eV.

Before the present study, accumulated photon echo experiments by using SR have been done at UVSOR for several organic molecules embedded in polymers as sample materials[1]. Excitation wavelengths were around 300 nm in these measurements. In the present study we extended excitation wavelength to about 200 nm and applied to inorganic crystals.

The experiment was done at BL8A of UVSOR. The experimental set-up was almost the same as in reference 1, except that the beam splitter was modified and the dispersion compensator was removed. The beam splitter used here consisted of two identical half mirrors. They were made by dividing equally a single half mirror and then mounted back-to-back so that their active surfaces are in one plane. The center of the excitation wavelength was selected by selecting appropriate combination of coatings of the beam steering mirrors and the beam splitter.

We tried echo measurement for two kinds of alkali-halide crystals as sample materials: RbI, KBr. The sample temperature was about 5 K. We tuned the excitation wavelength at the foot of the exciton absorption, which is 220 nm for RbI and 230 nm for KBr, and about half of the excitation energy was absorbed. The correlation time of the excitation was about 30 fs. We also tried a mixed crystal of RbI and KI at wavelength of 230 nm expecting a broad inhomogeneous distribution.

For the samples we tried we have not obtained any detectable echo signal. We do not know about he existence of bottleneck states in the present samples, and even less about their life times. Since fluorescence quantum yields are not so small in these samples, we can conclude at least that the bottleneck states do not effectively work in the present samples if any.

Reference

[1] H. Itoh *et al.*, UVSOR Activity Report 1996, 228(1997).

[BL-8A]

Temperature-dependent dephasing characteristics of Phenol doped in hosts and long-term phase stability of interferometer

H. Itoh[1], S. Nakanishi[1], T.Fuji[2], T.Kashiwagi[2], M.Furuichi[2], N. Tsurumachi[2], H. Nakatsuka[2], S. Asaka[3] and M. Kamada[4]

[1]*Department of Advanced Materials Science, Kagawa University, Takamatsu 760-8526*
[2]*Institute of Applied Physics, University of Tsukuba, Tsukuba 305-8573*
[3]*Equipment Development Center, Institute for Molecular Science, Okazaki 444-8585*
[4]*UVSOR, Institute for Molecular Science, Okazaki 444-8585*

We have applied synchrotron radiation (SR) to investigate FM-modulated incoherent accumulated photon echo signals of simple aromatic molecules doped in Polyvinyl Alcohol(PVA) and Polymethel Methacryrate in ultraviolet wavelength region. In this paper, we show two experimental results. One is precise temperature dependent phase relaxation of Phenol doped in PVA, relating to the relaxation way of Aniline doped in same host. On the other hand, signal intensities have extremely reduced since the latter half of last year. Then we check the reliability of our experimental apparatus to make its reason clear. The experiment was performed at BL-8A. The output beam from the quartz window of the BL-8A was filtered by the bandpass filter with the center wavelength of 289 nm, the bandwidth of about 12 nm and the maximum transmission rate of about 18%.

The temporal width of field autocorrelation was measured as 25 fs, corresponding to the bandpass filter used. In that time, to compensate the dispersion of the system, we inserted a quartz plate with 3 mm thick tilting by 34 degree of angle to the SR beam path between the PBS and one of the corner cube prisms. Figure 1 shows temperature dependent dephasing characteristics of Phenol doped in PVA as a function of inverse of temperature. The dephasing time of Phenol is longer as orders than that of the Aniline at the temperature around 4 K[1]. This dephasing characteristics would be originated from the interaction between the host and the guest molecules, such as TLS transition of host molecules, i.e. non-photochemical hole burning. Because this dephasing characteristic is inferred from the results, which have been investigated in many molecules doped in hosts in visible wavelength region. It is thought from this result that the dephasing mechanism for the Aniline/PVA would be slightly different from that of the Phenol/PVA system. The short dephasing time would reflect that the potential minimum of each ground and first excited state are shifted each other in normal coordinate, so that 0-0 transition of electro-vibronic states could not satisfy the Frank-Condon principle. Resulting from fast energy relaxation in excited state(internal conversion), phase coherence between ground and excited state is not maintained so long period.

Next we check long-term phase stability of the Michelson interferometer we used. Output SR beam from the interferometer was continuously detected by p-i-n photodiode when the interferometer's arm length was fixed at a position. At the same time, interference signal of a He-Ne laser was also detected by another p-i-n photodiode using same interferometer in the same geometry as the SR beam for investigating the stability of the Michelson interferometer alone. we show both intensities of interference lights as a function of time in Fig.2, solid and dotted line correspond to the signals by the SR light and He-Ne laser, respectively. The interference intensity of the SR drastically changed at random in short period according to the phase hopping from 0 to 180 degree. On the other hand, the intensity by the He-Ne laser did not change so drastically that the main instability factor is originated from spatial hopping of SR beam. This hopping of the SR beam erases holes burned in the sample. Since echo intensities are proportional to the depth of burned phase grating, we can not get fully accumulated signals. It is needed to keep, at least, this phase variation small in one round of the detecting period. It is thought that this hopping is caused from bad vacuum condition in beam line.

Reference

[1] H.Itoh et al. UVSOR Activity Report 1996.

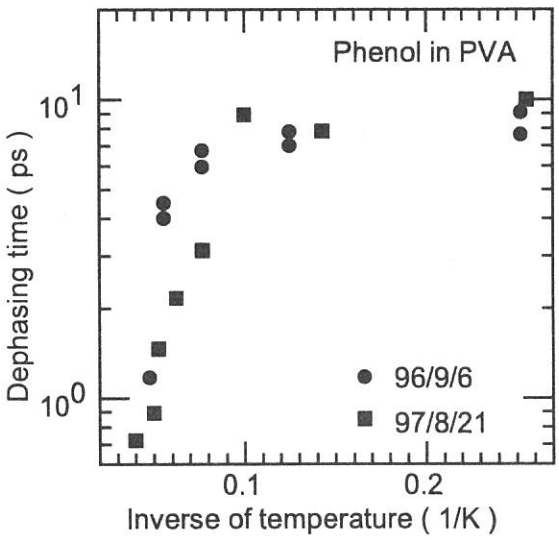

Fig. 1: Accumulated photon echo decay of Phenol doped in PVA as a function of inverse of temperature from 4.3 to 20K. The excitation wavelength is 289 nm with the bandwidth of about 12 nm. We show two results, circle denotes result of Sept.'96 and square corresponds to that of Aug.'97.

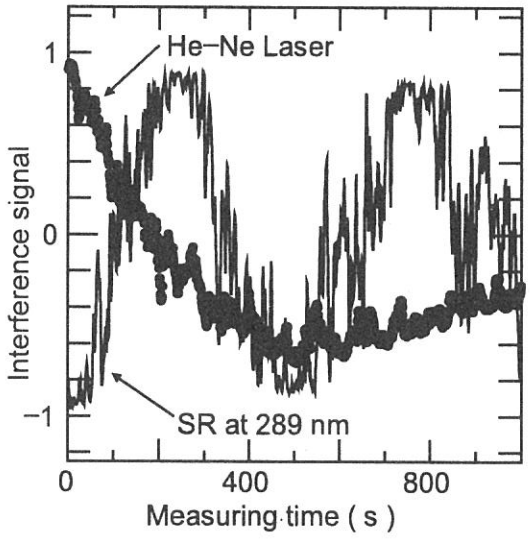

Fig. 2: Stability of interference signal with the path length in the Michelson interferometer fixed. Circle denotes the case of He-Ne laser and solid line corresponds to that of SR beam at 289 nm.

(BL1B & BL6A1)

Anisotropic reflectivity spectra of *R*PtAs (*R* = Ce, La)

S. Kimura, K.G. Nath[1], Y. Haruyama, T. Kinoshita, S. Yoshii[2] and M. Kasaya[2]

UVSOR Facility, Institute for Molecular Science, Okazaki 444-8585
[1]Department of Structural Molecular Science, The Graduate University for Advanced Studies, Okazaki 444-8585
[2]Department of Physics, Tohoku University, Aoba-ku, Sendai 980-8578

The crystal structure of CePtAs is hexagonal YPtAs-type ($P6_3/mmc$). The transport property along *c*-axis ($I \parallel c$) is semiconducting and that perpendicular to *c*-axis ($I \perp c$) is metallic. The Hall coefficient of $I \parallel c$ and $H \perp c$ is negative and small and that of $I \perp c$ and $H \parallel c$ is positive and large [1]. Here, *I* indicates current direction and *H* applied magnetic field. Therefore not only the shape of the Fermi surface and also the electronic structure attracts attention. In this study, we measured reflectivity spectra of CePtAs and of the reference material LaPtAs for the investigation of the electronic structure that makes the anisotropy of the transport and the mobility. The x-ray photoemission spectra (XPS) of valence band have also measured for the investigation of the occupied state.

The reflectivity spectra was measured at two beam lines of 1B and 6A1 for the measurements of visible - VUV (2 - 30 eV) and infrared (0.01 - 2 eV) regions, respectively. Obtained spectra of *R*PtAs are shown in Fig. 1. Anisotropy of reflectivity spectra is observed. XPS was measured by using a commercial system (FISONS Instruments, ESCALAB 220i-XL) and Mg-Kα line.

In figure 2, optical conductivity (OC) spectra of CePtAs with $E \perp c$ and $E \parallel c$ are shown. The OC spectra were determined from a Kramers-Kronig analysis of the reflectivity spectra. Optical anisotropy can be clearly observed in the whole photon energy region. Particularly, in the low energy part, the spectrum with $E \perp c$ shows metallic one because Drude type OC appears. On the other hand, the spectrum with $E \parallel c$ seems to be of a semiconductor. The result is consistent with the anisotropy of the electric resistivity.

Since the DC conductivity with $I \perp c$ at 300 K is $3.6\times10^3\ \Omega^{-1}\mathrm{cm}^{-1}$, the Drude curve of the OC with $E \perp c$ is considered to connect to DC smoothly.

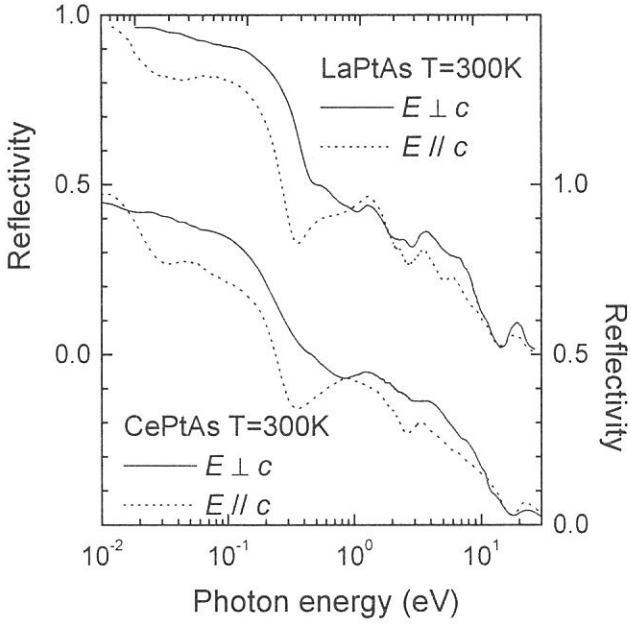

Fig. 1. Anisotropic reflectivity spectra of *R*PtAs (*R* = La, Ce) in the energy range of 0.01 - 30 eV.

And also, the OC with E // c smoothly connected to the DC conductivity with I // c because the DC conductivity is about 0.37×10^3 $\Omega^{-1}cm^{-1}$. The energies of the plasma edges with $E \perp c$ and with E // c are about 0.3 eV and about 0.03eV, respectively. Generally square of energy of plasma edge is proportional to the effective carrier density ($N\times m_0/m^*$, where N is the carrier density, m_0 the static mass of an electron and m^* the effective mass). Therefore the effective carrier density with $E \perp c$ is hundred times higher than that with E // c. Therefore the mobility (effective mass) with $E \perp c$ is hundred times larger than that with E // c. This is an origin of the anisotropy of physical properties of CePtAs.

Higher energy part of OC spectra and XPS of CePtAs are shown in Fig. 3. The binding energy of XPS is shifted by 0.5 eV from the photon energy of OC spectra. Double peak structure at 4 and 5 eV of XPS mainly originates from Pt 5*d* state. Therefore the shape of OC around 4 eV is due to the charge transfer excitation of Pt $5d \rightarrow$ Ce $4f$. The shape of the reflectivity spectra of LaPtAs around 4 eV is sharper than that of CePtAs in Fig. 1. Since the multiplet structure of $4f^2$ final state of Ce^{3+} after photo absorption is wider than that of $4f^1$ final state of La^{3+}, the difference appears in the reflectivity spectra.

---

[1] S. Yoshii et al., Proc. Int. Conf. Magn. 97. (to appear in J. Magn. Magn. Mater.)

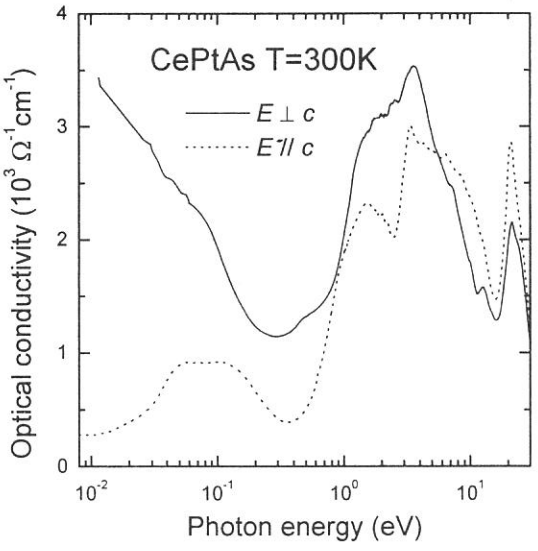

Fig. 2. Anisotropic optical conductivity of CePtAs. The spectrum with $E \perp c$ shows metallic one but that with E // c looks like an insulator.

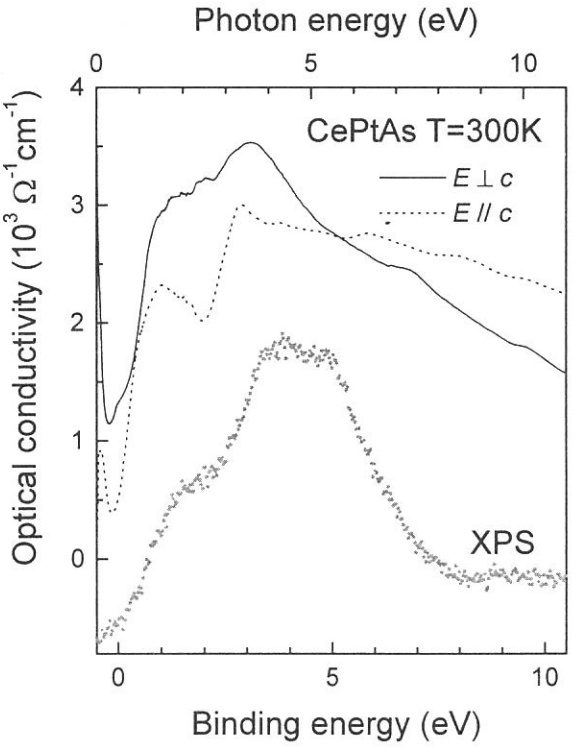

Fig. 3. Comparison of optical conductivity spectra of CePtAs with the valence band photoemission spectrum. The binding energy of photoemission spectrum shifted by 0.5 eV from the photon energy of optical conductivity spectra.

(BL-1B)

Determination of Threshold Energy of Color Center Formation in Anthracene Single Crystal

Iwao Shimoyama and [1] Kazumichi Nakagawa

Graduate School of Sci. and Tech., Kobe University, Rokkohdai, Nada-Ku, Kobe 657, Japan
[1]Faculty of Human Development, Kobe University, Tsurukabuto, Nada-Ku, Kobe657, Japan

Anthracene single crystal is a standard for radiation scintillator. Scintillation efficiency is known to be degraded by radiation induced color centers. However the detail of radiation damage of anthracene has not known yet. To clarify the lowest excitation state form which color centers are produced, we measured quenching of fluorescence of S_1 exciton as a function of irradiation time and determine the threshold energy of color center formation.

Experiments were performed at BL-1B. Anthracene crystals were grown by sublimation method from scintillation grade anthracene powder of Kantou Kagaku Company after purification by zone melting method. Samples were placed in vacuum chamber (10^{-8}Torr) and cooled at 200K. We used fluorescence quenching technique (FQT). In FQT, at first, fluorescence intensity $I_F(0)$ induced by 365nm light and intensity M of 365nm light is measured before VUV irradiation. The 365nm light is known to produce S_1 exciton and not to produce color centers. Fluctuation in the value of $I_F(0)/M$ was confirmed to be less than 1% during 110 minutes (see figure 1). Next, the sample were irradiated by VUV with various energies ($h\nu$ = 9.0, 9.5, 10, 10.8, 13.7 and 17.7 eV) during T seconds. After stopping VUV irradiation, we measured $I_F(T)/M$ as a function of T. We estimated irradiation photon numbers N_λ ($= I_\lambda T$) by measuring incident photon numbers I_λ per second. And we obtained S_1 quenching rate $I_F(N_\lambda)/I_F(0)$ as a function of N_λ. Figure 2 shows $I_F(N_\lambda)/I_F(0)$ plots for irradiation of VUV with the energies 9.0(●), 9.5(△) and 10eV(■). In the case of 9.0, $I_F(N_\lambda)/I_F(0)$ shows no quenching. Therefore we concluded that color center isn't formed at this photon energy. In the case of 9.5 eV, $I_F(N_\lambda)/I_F(0)$ shows just small values near $N_\lambda = 4\sim5\times10^{14}$ [photons]. However the data doesn't show systematically decrease, therefore we couldn't conclude whether color center is formed or not at this photon energy. While, in the case of 10eV, $I_F(N_\lambda)/I_F(0)$ decrease apparently. In other cases that photon energy are larger than 10eV, we also obtained apparent decrease of $I_F(N_\lambda)/I_F(0)$. Therefore we concluded that the threshold energy of color center formation is about 9.5eV.

It is considered that C-H bond dissociation is important reaction to form color center. For anthracene vapor, C-H bond assignment has reported only in the energy region 5～8.5 eV. In an

assignment of benzene vapor reported by Koch *et al.* [1], the highest C-H bond is assigned to 11eV, we couldn't also find C-H bond near 9.5eV. From our result, the transition energy which concern C-H bond should be near 9.5 eV. This result seems to indicate the possibility of new theory for molecular orbital calculation.

[1] E. E. Koch and A. Otto, Chem. Phys. Lett., 21,501(1973)

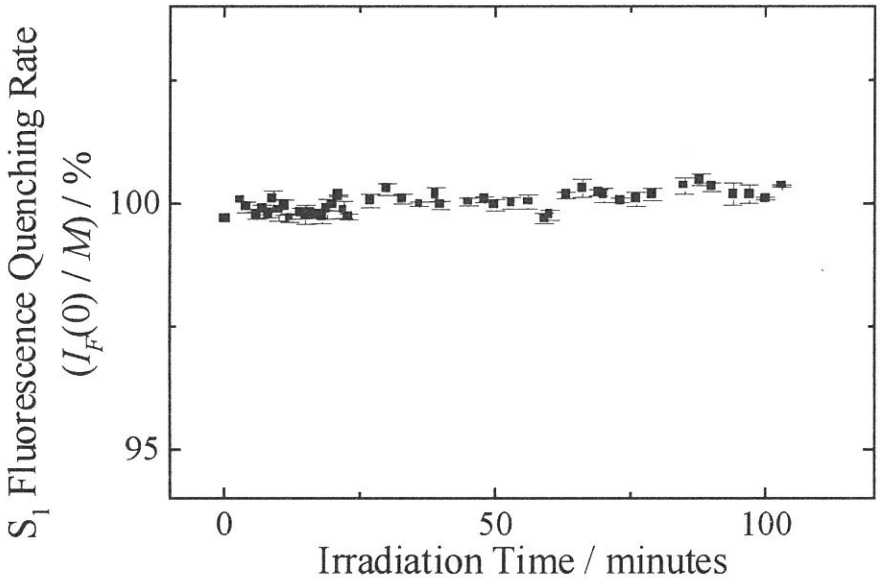

Figure 1. Stability of $I_F(0) / M$

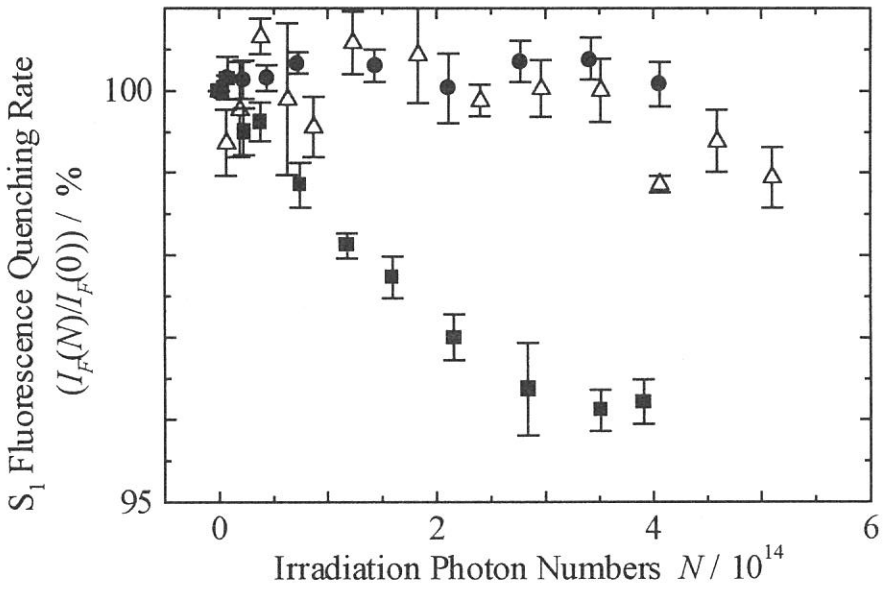

Figure 2. S1 quenching rate $I_F(T) / I_F(0)$

$h\nu$ = ● : 9.0, △ : 9.5, ■ : 10eV

(BL1B)

VUV~UV absorption spectra of thermally poled synthetic silica glass

Akihiro Kameyama, Atsushi Yokotani and Kou Kurosawa

Department of E&E Engineering, Miyazaki University, Miyazaki 889-2155

Silica glass has become much more important and also attractive for photonics engineering, because a new function of a permanent strong second-order optical nonlinearity has been observed in poled silica glass in addition to high transparency and high band-gap energy. Although the optical nonlinearity is as high as 1 pm/V in thermally poled fused silica glass by Myers et al.[1], the optical nonlinearity in thermally poled synthetic silica was about one order of magnitude smaller than in the fused silica one. We have reported[2] that the large second order nonlinearity of 0.2pm/V in high-purity synthetic silica glass exposed to X-ray before the poling procedures. Furthermore we have observed that the large second order nonlinearity in high-purity synthetic silica glass with KrF excimer laser exposure before the poling procedures. The radiation-induced defects seem to be important for the generation of second order nonlinearity.

In order to identify the defects relevant to the generation, we observed VUV absorption spectra for the poled synthetic silica glass with KrF excimer laser exposure before the poling procedures.

We used samples of synthetic silica glass supplied from Nippon Silica Glass. The samples have a plate-like shape with 20 mm in diameter and 1.5 mm in thickness and the surface were finished to optical quality. The samples were exposed to 248-nm pulses of 10000 shots of 50 mJ/cm^2 from a KrF excimer laser. The poling procedures were as follows: A sample plate was sandwiched with two electrodes maintained at a high voltage of 4.5 kV, heated up to 260°C at the rate of 10°C/min, held for 20 min, and then cooled down to room temperature at the rate of 10°C/min before removing the voltage.

In Fig. 1 are plotted SHG intensities as function of incident angle of Nd:YAG laser beam observed in the poled synthetic silica with and without the laser irradiation. The SHG intensity was observed only in the exposed sample, but not in the non-exposed sample.

We observed absorption spectra with the use of BL1B beam line at UVSOR. In Fig. 2 are shown transmittance spectra taken from samples with and without the KrF excimer laser exposure. The laser radiation apparently decreases a 6.3-eV absorption peak which is assigned to E'center, and further increases significantly a 4.7-eV absorption peak which is probably to be NBOHC (≡Si-O*) or ≡Si-O$^-$.The photon energy of 5.0 eV is very close to the center energy of absorption bands. Such speculation agrees with the result the X-ray irradiation experiments[2], namely ≡Si-O* or ≡Si-O$^-$ induced in high purity silica glass and to be close-related with the nonlinearity creation.

In summary, we investigated a VUV absorption spectra of the poled synthetic silica glass with KrF excimer laser exposure before the poling procedures. We conclude that the optical nonlinearity include defects related with Si-O at least in pure silica glasses.

Reference
1) R.A.Myers, N.Mukherjee, and S.R.J. Brueck, Opt. Lett. 16, 1732 (1991).
2) A.Kameyama, E.Muroi, A.Yokotani, K.Kurosawa and P.Herman,
J.Opt.Soc.Am. B, 14, 1088 (1997).

Fig. 1 The SHG intensities as function of incident angle of YAG laser beam in the thermally poled silica glass with (●) and without (■) KrF excimer laser exposure.

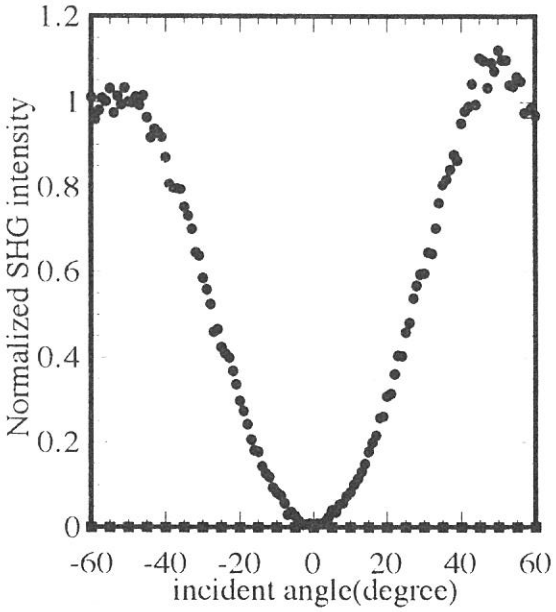

Fig. 2 Transmittance spectra taken from silica glass with (●) and without (■) KrF excimer laser exposure.

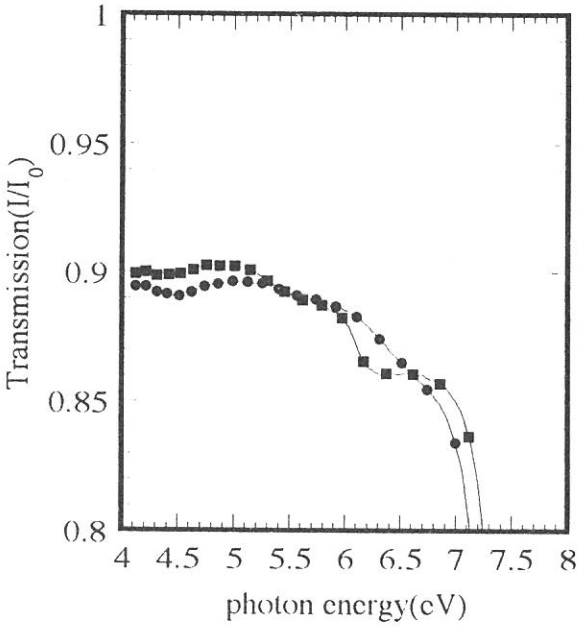

(BL1B)

Concentration of neutral oxygen vacancies in buried oxide formed by implantation of oxygen

K. S. Seol, T. Futami, and Y. Ohki

Department of Electrical, Electronics, and Computer engineering, Waseda University, 3-4-1 Ohkubo, Shinjuku-ku, Tokyo 169

Buried oxide layers in the silicon-on-insulator structure separated by implanted oxygens (SIMOX) have become widely used for a high speed metal oxide semiconductor (MOS), a radiation-hardened complementary MOS (CMOS), and other smart devices.[1,2] Many researches have been done recently on the nature of the buried oxide[3], since it plays an important role in determining the device properties. It has been considered that the buried oxide is far more oxygen-deficient than the conventional thermal oxide,[3] and that this deficiency is believed as one reason of unusual behavior of buried oxide such as enhanced electrical conductivity, charge buildup, and sensitivity to defect generation.[3]

It has been known that buried oxide contains neutral oxygen vacancies ($O_3{\equiv}Si\text{-}Si{\equiv}O_3$) which are typical in oxygen-deficient amorphous SiO_2.[4] In this study, the vacancy concentration in buried oxide is estimated by measuring the PL intensity.

In any material, the concentration (N) of photo-absorbing defects can be easily estimated from the following equation by measuring the optical absorbance (A) if their absorption cross section (σ) and the sample thickness (L) are known:

$$A = L\alpha = L\sigma N , \qquad (1)$$

where α is the optical absorption coefficient. However, in the case of the present buried oxide sample, it is impossible to measure A because of the opaqueness of the Si substrate. One possible method to estimate the concentration of oxygen vacancies is to measure the PL emitted from the vacancies. It is known that the 4.3-4.4 eV PL is the luminescence from the vacancies[5] and that its two excitation bands at 5.0 and 7.6 eV are due to absorptions by '*unrelaxed*' and '*relaxed*' oxygen vacancies, respectively.[6] Here, the unrelaxed vacancy has a larger bond length between the two silicons and the relaxed vacancy has a shorter one.[6] The PL intensity (I_{PL}) normalized by the excitation photon intensity (I_{EXC}) is given by,[5]

$$I_{PL} / I_{EXC} = \eta \cdot (1 - \exp(-\alpha L)) . \qquad (2)$$

Here, η is the quantum efficiency of the PL. It is reasonable to assume that the true quantum efficiency for a specific PL by a specific PL excitation band, namely the PL photon number induced by a certain number of incident photons, is independent of the sample whether it is a thick silica glass or a thin buried oxide layer. Of course, such a true efficiency cannot be measured in actual experiments. First, since I_{EXC} was measured with a photomultiplier coated with sodium salicylate whose fluorescent quantum yield is constant between 4 and 20 eV,[7] I_{EXC} in the present research represents only a relative number of the incident photons. Secondly, although all the experimental conditions such as the configuration of photo-detecting systems were exactly the same for the two samples, the two samples differ in the point that the buried oxide layer has a Si substrate at its back. Some of the incident photons, which should pass through the silica glass, could be reflected by the Si substrate. Reflectance at the interface between crystalline Si and vacuum is reported to be 60-70 % at 4.3, 5.0, and 7.6 eV.[8] The reflectance at the present SiO_2/Si interface should be somewhat smaller, while the reflectance at SiO_2/vacuum interface could be assumed zero. The reflectance at SiO_2/Si increases not only the effective incident photons but also the effective PL intensity. Therefore, if the reflectance at the SiO_2/Si interface is assumed to be 60 %, the effective value of η for the buried oxide sample becomes $(1.6)^2$ times as high as that for the silica glass.

PL intensities was first measured for an oxygen-deficient silica glass, the α value of which had been calculated by measuring the absorbance. Then, under the same condition, PL intensities were measured on the buried oxide layer. The PL measurement was carried out at 13 K using synchrotron radiation at the Institute for Molecular Science, Okazaki, Japan. The investigated silica glass was manufactured by the soot remelting method and its thickness is 0.7 mm. The SIMOX sample was fabricated by implanting O^+ ions up to a dose of $3.7{\times}10^{17}$ cm^{-2} with an energy of 180 keV into a Si substrate, and subsequent annealing in an Ar atmosphere followed by oxidation at 1350 °C for several hours. The thickness of the buried oxide layer is about 130 nm. For the PL measurement, the thermal oxide and the Si layer over the buried oxide were respectively removed by soaking the sample in a HF solution and subsequently in a KOH solution.

Figure 1 shows the PL spectra from the buried oxide layer excited by 5.0 and 7.6 eV photons. The PL band with a peak at 4.3-4.4 eV appears regardless of the excitation photon energy. The PL intensity shown in Fig. 1 was calibrated by taking the intensity variation of the excitation photons into consideration. Quite similar PL spectra were obtained for the glass sample. The measured apparent values of I_{PL}/I_{EXC} excited at the 5.0 eV excitation band and at the 7.6 eV band are respectively 2.0×10^{-4} and 1.1×10^{-4} for the glass sample, while they are respectively 2.6×10^{-5} and 4.8×10^{-5} for the buried oxide layer. The values of the absorption coefficient α of the glass sample are calculated to be 7.0×10^{-3} cm^{-1} and 24 cm^{-1} at 5.0 eV and 7.6 eV, respectively, by measuring the absorbance A at each photon energy. Then, by substituting the values of I_{PL}/I_{EXC}, α, and L into Eq. (2), the value of η for the silica glass measured with the present system is calculated to be 4.0×10^{-1} and 1.4×10^{-4} for the 5.0 eV photons and the 7.6 eV photons, respectively. As mentioned above, the effective values of η for the buried oxide layer are considered to be $(1.6)^2$ times as high as these values. If so, using the values of I_{PL}/I_{EXC} and L for the buried oxide layer, α can be obtained as 2.0 for the 5.0 eV absorption band and 1.1×10^{4} for the 7.6 eV band. Since σ is known to be 2×10^{-17} cm^2 and 8×10^{-17} cm^2 for the 5.0 eV and the 7.6 eV bands, respectively,[6] the concentration N of the photo-absorbing defects in the present buried oxide layer is calculated to be 1.0×10^{17} cm^{-3} for the unrelaxed neutral oxygen vacancies and 1.4×10^{20} cm^{-3} for the relaxed ones. The concentrations in the glass sample are similarly calculated to be 3.5×10^{14} cm^{-3} and 3.0×10^{17} cm^{-3} for the unrelaxed and the relaxed vacancies, respectively. It can be concluded that the vacancy concentrations in the buried oxide layer are about 300 - 400 times as high as those in the glass sample.

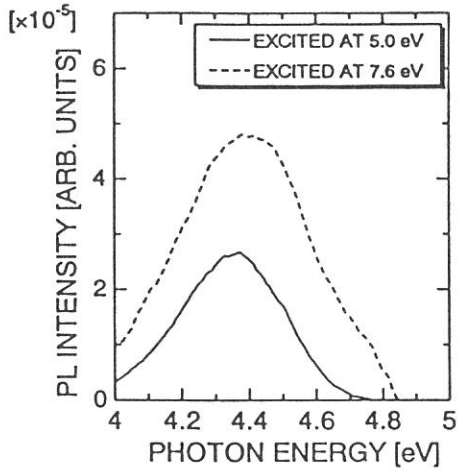

FIG. 1. PL spectra excited by 5.0 and 7.6 eV photons measured for the buried oxide layer at 13K. The PL intensity is calibrated by the intensity of excitation photons.

References

1. Y. Omura and K. Izumi, in *Proceedings of the 4th International Symposium on Silicon-on-Insulator Technology and Devices*, edited by D.N. Schmidt, PV 90-6 (The Electrochemical Society Proceedings Series, Pennington, NJ, 1990), p. 509.
2. T. Ohno, M. Shimaya, K. Izumi, and N. Shiono, IEEE Trans. Circuits Devices, CD-3, 21 (1986).
3. For example, A.G. Revesz and H.L. Hughes, Microelec. Eng. 36, 343 (1997), K. Vanheusden and A. Stesmans, Appl. Phys. Lett. 62, 2405 (1993).
4. K.S. Seol, A. Ieki, and Y. Ohki, J. Appl. Phys. 79, 412 (1996).
5. H. Nishikawa, E. Watanabe, D. Ito, and Y. Ohki, Phys. Rev. Lett. 72, 2101 (1994).
6. H. Imai, K. Arai, H. Imagawa, H. Hosono, and Y. Abe, Phys. Rev. B 38, 12772 (1988).
7. R. Allison, J. Burns, and A.J. Tuzzolino, J. Opt. Soc. Am. 54, 747 (1964).
8. H.R. Philipp, J. Phys. Chem. Solids 32, 1935 (1971).

(BL1B)

Reflection Spectra of $(CH_3NH_3)_3M_2Br_9$ (M:Sb,Bi) Single Crystals

Taketoshi Kawai[A], Akira Miyashita[B] and Makoto Iwata[B]

[A]*Department of Natural Science, Osaka Women's University, Daisen−cho, Sakai 590-0035, Japan*

[B]*Department of Applied Physics, Nagoya University, Nagoya 464-8603, Japan*

Novel crystals of alkylammonium halogenometallates $(CH_3NH_3)_3M_2X_9$ (M=Sb,Bi: X=Cl,Br,I) which contain the trivalent ion as the constituent metal exhibit several interesting structure phase transitions mainly due to the ordering of orientational motion of alkylammonium cations with the permanent dipole moment. Therefore, a number of studies on these materials have been extensively made on phase transitions and dielectric properties[1-5]. On the other hand, there are only few studies on optical properties of these novel crystals[6]. We have investigated the optical properties of the bromo derivatives $(CH_3NH_3)_3Sb_2Br_9$ (MABA) and $(CH_3NH_3)_3Bi_2Br_9$ (MABB) in the photon energy of 2.0～24eV. The compounds have a corrugated layer of the inorganic $[(M_2Br_9)^{3-}]_n$ polyanions and the $(CH_3NH_3)^+$ cations occupying the vacancies.

Single crystals of MABB and MABA were grown by slow evaporation of the HBr solution containing the stoichiometric molar ratio of Bi_2O_3 or Sb_2O_3 and CH_3NH_3Br. The obtained crystals have the form of hexagonal plates of transparent yellow color. They were cleaved along the crystallographic *ab*-plane in order to use as a reflection plane. The reflection spectra at near-normal incidence were measured at the beam line BL1B of UVSOR by using a monochromator of 1m Seya-Namioka type. The measurements were performed in the temperature range from 300K to 8K, because both crystals exhibit several structure phase transitions in this temperature range.

Figures 1(a) and 1(b) show the reflection spectra of the MABB and MABA single crystals at several temperature in the energy region of 2.0～6.0eV, respectively. As seen in these figures, several remarkable structures were observed in this energy region. The rapid drop structure at 2.73eV for MABB and 2.85eV for MABA is correspond to the energy position which each absorption spectrum exhibits a steep rise. Thus, the rapid drop structures are probably due to the reflection from the back surface of the crystals. At low temperature, the sharp reflection structure at 2.90eV for MABB and 2.95eV for MABA is attributed to the band-edge exciton state. Since the CH_3NH_3Br solution does not exhibit any absorption band in the energy region below 6.0eV, the origin of the electronic states may be interpreted on the basis of electronic states in the metal cation. Preliminary analysis of the reflection structure by the simple oscillator model provide the following values for the band-edge exciton. The transverse exciton energy and the longitudinal- transverse splitting energy are 2.90eV and 80meV for MABB, and 2.95eV and 60meV for MABA, respectively.

As the temperature increases, the reflection structures red-shift and become broader gradually. The MABB and MABA crystals have the phase transition temperatures of about 101.5, 140 and 188 K, and about 130 and 168 K, respectively. The drastic change of the reflection spectra is not observed at any phase transition temperature. This result supports that the band-edge exciton states have it's origin in electronic states in the metal ion, because the orientational motion of the $(CH_3NH_3)^+$ cations

(BL1B)

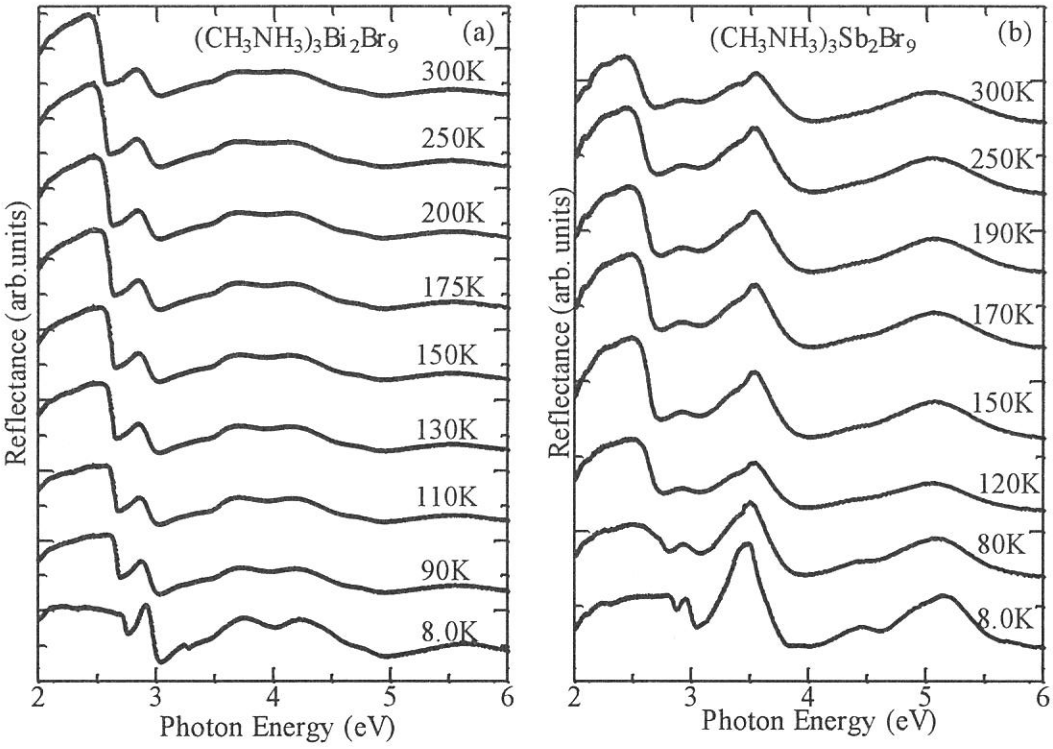

Figure 1 Reflection spectra of MABB (a) and MABA (b) at various temperature.

is not considered to distort the framework of the inorganic $[(M_2Br_9)^{3-}]_n$ polyanions. It should be noticed that the reflection peak in MABB is clearly observed even at 300K. On the other hand, the structure in MABA is hardly observed at 300K. This fact means that the band-edge exciton in MABB has a large binding energy in comparison with that in MABA. The quantitative analysis including the temperature dependence of the reflection structure in the higher energy is now in progress.

References

[1] R.Jakubas and L.Sobczyk: Phase Transitions **20** (1990) 163.

[2] R.Jakubas, Z.Galewski, L.Sobczyk and J.Matuszewski: J.Phys.C **18** (1985) L857.

[3] R.Jakubas, U.Krzewska, G.Bator and L.Sobczyk: Ferroelectrics **77** (1988) 129.

[4] P.Koziol, Y.Furukawa and D.Nakamura: J.Phys.Soc.Jpn **60** (1991) 3850.

[5] M.Iwata, M.Eguchi, Y.Ishibashi, S.Sasaki, H.Shimizu, T.Kawai and S.Shimanuki: J.Phys.Soc.Jpn **62** (1993) 3315.

[6] T.Kawai, A.Ishii, T.Kitamura, S.Shimanuki, M.Iwata and Y.Ishibashi: J.Phys.Soc.Jpn **65** (1996) 1464.

(BL1B)

Optical Properties of Cerium-doped Oxide and Fluoride Crystals for Laser Media I

Yoshiro SUZUKI, Hisashi UMEDA, Tooru HIRAYAMA and Kiyoshi INOUE
Faculty of Engineering, Tohoku University, Aoba, Sendai, 980-77

Introduction

Optical properties of cerium-doped materials have received considerable interests in recent years in connection with the application to tunable solid state laser media. [1] Several reports were made on the laser activity of cerium-doped fluoride crystals in UV region, while none of oxide crystals in visible region. This is believed to be due to optical losses by what is called the excited state absorption.[2] The excited state absorption is attributed to the transition from the lowest 5d excited state of the trivalent cerium ions (Ce^{3+}) to the conduction band of the host materials. Therefore, it is important to determine the location of the energy levels of the Ce^{3+} in the band gap for prediction of the laser activity. However, quantitative nor systematic evaluation has hardly been made because of lacking of the fundamental data.

As the first step, the measurements of the reflection spectra and the excitation spectra of the Ce^{3+} emission in several laser crystals have been carried out in the photon energy range of 4 to 17eV in order to obtain the information on the band gap energies.

Experimental

Crystals of $Y_3Al_5O_{12}$ (YAG) containing cerium were grown by Czochralski method in Tokin Inc., while those of $Gd_3Sc_2Ga_3O_{12}$ (GSGG), $YAlO_3$ (YAP), $YLiF_4$ (YLF) were furnished by the courtesy of Dr.Y.Segawa of Photodynamics Research Center, the Institute of Physical and Chemical Research. The crystals of YAP and YLF are anisotropic , then their orientations were determined through a comparison of the polarized absorption spectra with those from the literature.[3,4] The orientation of the crystals and the nominal concentrations of the Ce^{3+} are presented in each frame of Fig. 1.

The measurements were carried out at room temperature. The spectra of the reflection and the excitation of Ce^{3+} emission were measured by means of a Seya-Namioka-type VUV monochromator at the beam line BL1B. The band width for the reflection and the excitation spectra was 0.1 and 0.3nm,respectively. The reflected and emitted light were detected both at angle of 45° with the incident direction.

Experimental Results and Discussion

Solid curves in Fig.1 show the reflection spectra of the respective crystals. The measured reflectivity are normalized to the reflectance calculated using the refractive indices in the transparent region.[5] The reflection spectra were analyzed using Kramers-Kronig relationship by Roessler method.[6] Chain curves in Fig.1 present the imaginary part of the dielectric function, ε_2 thus obtained. The ε_2 spectra of YAG and YAP are essentially similar to those previously reported.[7,8] The main peaks at 9.0eV in YAG and 8.7eV in YAP were assigned to the transitions from the $O^{2-}2p^6$ to $Y^{2+}4p^6(4d+5s)$ level.[8] The structures due to exciton peaks are obscure at the leading edges of 6 to 8eV. This is characteristic manifestation in complex oxide crystals and attributed to the broadening and overlapping of multiple exciton absorption due to large atomic numbers in the unit cell.[9] The same feature is the case in GSGG and YLF. Therefore, it is difficult to determine the band gap energies only from the ε_2 spectra.

Dashed curves in Fig.1 show the excitation spectra of Ce^{3+} emission, which is caused by the transition from the lowest 5d excited state to the 4f ground state of the Ce^{3+}. The emission was detected at around the peak energy of the emission band in the respective crystals; 2.1eV in YAG and GSGG, 3.3eV in YAP and 3.8eV in YLF. The several bands due to the intraionic excitation to the higher lying 5d states are observed below 6.0eV in YAG and GSGG, while 7.0eV in YAP and YLF. Notable are the bands located around the leading edge of the fundamental absorption of the respective crystals; 6.8 to 8.0eV in YAG, 6.0 to 7.0eV in GSGG, 7.9eV in YAP and 10.3eV in YLF. These are denoted by the edge bands hereafter. Tomiki et al. reported the excitation spectra of Ce^{3+} emission from YAG:Ce and YAP:Ce powder phosphors and suggested the exciton formation by the intrinsic tail excitation.[8] Murk et al. detected the emission due to self trapped excitons (STE) in undoped YAG and YAP.[10] The excitation spectra of STE emission are very similar to the edge bands of YAG and YAP. This suggests the energy transfer from STE to Ce^{3+} and supports the exciton as the origin of the edge bands. It follows that the fallings at the high energy side of the edge bands are interpreted from the decrease of the transfer efficiency due to photoionization. The increase of the reflection loss contributes insignificantly to the falling. Figure 1 shows 40 to 90 % decreases in excitation intensity at the high energy side of the edge bands, whereas only 11 to 18% increases in reflectance is observed in the identical energy regions. Then, we may obtain indication of the electron-hole

continuum excitation from the falling edge energies of the edge bands in the respective crystals ; 8.0eV in YAG, 6.8eV in GSGG, 7.8eV in YAP and 10.5eV in YLF. It is consistent that these energies correspond to the singular points of the ε_2 spectra where steeper rises are observed. The band gap energy of YAG was determined to be 8.0eV from a photocurrent measurement.[11] The agreement with the falling edge energy of the edge band in YAG supports the validity of the falling edge as an indicator of the continuum excitation.

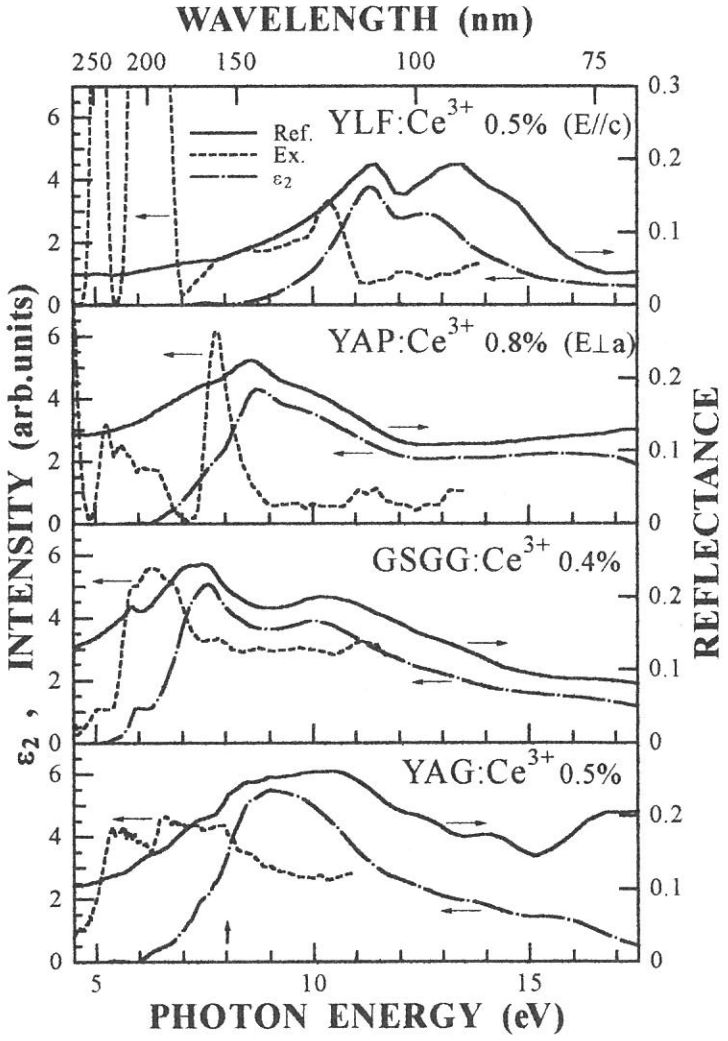

Fig.1 Spectra of Ce doped YAG, GSGG, YAP and YLF at room temperature : reflection (solid), ε_2 (chain) and excitation spectra of the Ce^{3+} emission (dashed curves) .

References

[1] See, for example, N.Sarukura : Kogaku, **25** (1996) 518 [in Japanese] .

[2] D. S. Hamilton et al. : Phys. Rev. **B 39** (1989) 8807.

[3] S. Yan, G. Yuan and Y. Zhong : Materials Lett. **16** (1993) 222.

[4] N. Sarukura et al. : IEEE J. Selected Topics in Quantum Electronics, **1** (1995) 792.

[5] L. G. DeShazer et al. : CRC Handbook of Laser Science and Technology, ed. M. J. Weber (CRC Press, Boca Raton Fla.1987) Vol. 5, p. 281.

[6] D. M. Roessler : Br. J. Appl. Phys. **16** (1965) 1119.

[7] V. N. Abramov and A. I. Kuznetsov : Sov. Phys. Solid State **20** (1978) 399.

[8] T. Tomiki et al. : J. Lumin. **40 & 41** (1988) 379.

[9] A. I. Kuznetsov et al. : Trudy Inst. Fiz. Akad. Nauk. Est. SSR. **63** (1989) 19.

[10] V. Mürk et al. : Nucl. Instrum & Methods Phys. Research **B 91** (1994) 327.

[11] N. S. Rooze and N. A. Anisimov : Trudy Inst. Fiz. Akad. Nauk. Est. SSR. **44** (1975) 163.

(BL1B)

Optical Properties of Cerium-doped Oxide and Fluoride Crystals for Laser Media II

Yoshiro SUZUKI, Hisashi UMEDA, Tooru HIRAYAMA and Kiyoshi INOUE
Faculty of Engineering, Tohoku University, Aoba, Sendai, 980-77

Introduction

Cerium-doped materials have received much attention as tunable solid state laser media. [1] The emission due to the transition from the lowest 5d excited state ($5d^1$) to the 4f ground state of the trivalent cerium ions (Ce^{3+}) is used for the laser action. The peak energy of Ce^{3+} emission varies from UV to visible region depending on the host materials. Up to date, however, the tunable energies of Ce^{3+} laser are restricted to UV region using fluoride crystals. The visible laser action using oxide crystals is believed to be hampered by so-called excited state absorption. [2] Since the excited state absorption is attributed to the transition from the $5d_1$ state to the conduction band of the host materials, the location of the energy levels of the Ce^{3+} in the band gap is crucial for the laser activity.

In the preceding report,[3] we showed that the excitation spectra of Ce^{3+} emission in VUV region give information of the band gap energies of the host crystals. In the present study, the measurements have been extended to UV and visible regions where intraionic transitions of the Ce^{3+} are observable. The quantum efficiencies of Ce^{3+} emission are known to be almost unity under the $5d_1$ excitations,[4] while those under the higher 5d excitations are unknown. Since the latter excitations may cause electron-release to the conduction band and reduce the quantum efficiency, the excitation spectra of Ce^{3+} emission have been expected to give information of the energy separation between the 4f ground state of the Ce^{3+} and the bottom of the conduction band.

Experimental

Cerium-doped crystals of $Y_3Al_5O_{12}$ (YAG), $Gd_3Sc_2Ga_3O_{12}$ (GSGG), $YAlO_3$ (YAP), $YLiF_4$ (YLF) were identical with those in the preceding report.[3] Presented in each frame of Fig.1 are the thickness and the nominal concentrations of the Ce^{3+} of the respective crystals, as well as the crystal orientation if anisotropic.

The measurements were carried out at room temperature. The excitation spectra of Ce^{3+} emission above 3.5eVwere measured at the beam line BL1B in the identical optical configuration with those in the preceding report.[3] The sufficient beam intensities facilitated the measurements and their corrections. The excitation spectra below 3.5eV were measured with a conventional optical system using a Xe lamp, since the sodium salicylate scintillater was unavailable at these energies. The absorptivity spectra of the respective crystals were also measured in order to evaluate the quantum efficiencies through comparisons with the excitation spectra. The band widths for the excitation and the absorption spectra above 3.5 eV were both 0.3nm, while those below 3.5 eV were 1.5nm.

Experimental Results and Discussion

Solid curves in Fig.1 show the absorptivity spectra of the respective crystals. The reflection losses were not corrected, while the absorbance at the transparent region were subtracted as the background. Several absorption bands observed are due to the transition from the 4f ground state to the crystal-field levels of the 5d excited states of the Ce^{3+}. The increased covalency and crystal field in oxide crystals gives the red shifts of the absorption peaks compared with those in YLF. Absorption tails due to the anisovalent cerium ions or the other impurities are obvious at the high energy region in GSGG and YAP.

Dotted curves in Fig.1 show the emission spectra under the $5d_1$ excitation. The doublet structure prominent in YLF is due to the spin-orbit splitting of the 4f ground state. The broadening of the emission bands in oxide crystals makes the structure obscure.

Dashed curves in Fig.1 show the excitation spectra of Ce^{3+} emission detected at around the peak energy of the emission band in the respective crystals. The heights were normalized to the peak heights of the $5d_1$ absorption bands. It is evident that the excitation spectra almost follow the absorptivity spectra in the whole energy region in YAG and YLF. Although the excitation spectra in GSGG and YAP apparently slip down from the absorptivity spectra at the higher energy region, the absorption tails due to the anisovalent cerium ions or the other impurities seem to be responsible for the disagreements. These behaviors of the excitation spectra of Ce^{3+} emission are unexpected. The photoionization threshold energy of the Ce^{3+} in YAG was determined to be 3.8eV from a photocurrent measurement.[5] However, no manifestation of the photoionization is observable in the present excitation spectra around 3.8 eV in YAG. The present result of YAG is not consistent with the previous one by Tomiki et al. either.[6] They reported that the relative intensity of the excitation band of Ce^{3+} emission to that of the absorption band decreased drastically at higher energy region. The reason of this discrepancy is not clear. The emission quenching may depend on the concentration of the electron-trap competitive with the photoionized Ce^{3+}.

Codoping of the electron-trap ions might be necessary for the observation of the photoionization threshold.

On the other hand, the spectral dependence of the excitation spectra is desirable for the laser performance. The Ce^{3+} is usually excited to higher lying 5d states in the laser performance because of less variety of pumping sources. The present result suggests that the Ce^{3+} emission efficiency does not decrease under such excitation as far as multiphoton processes are not induced.

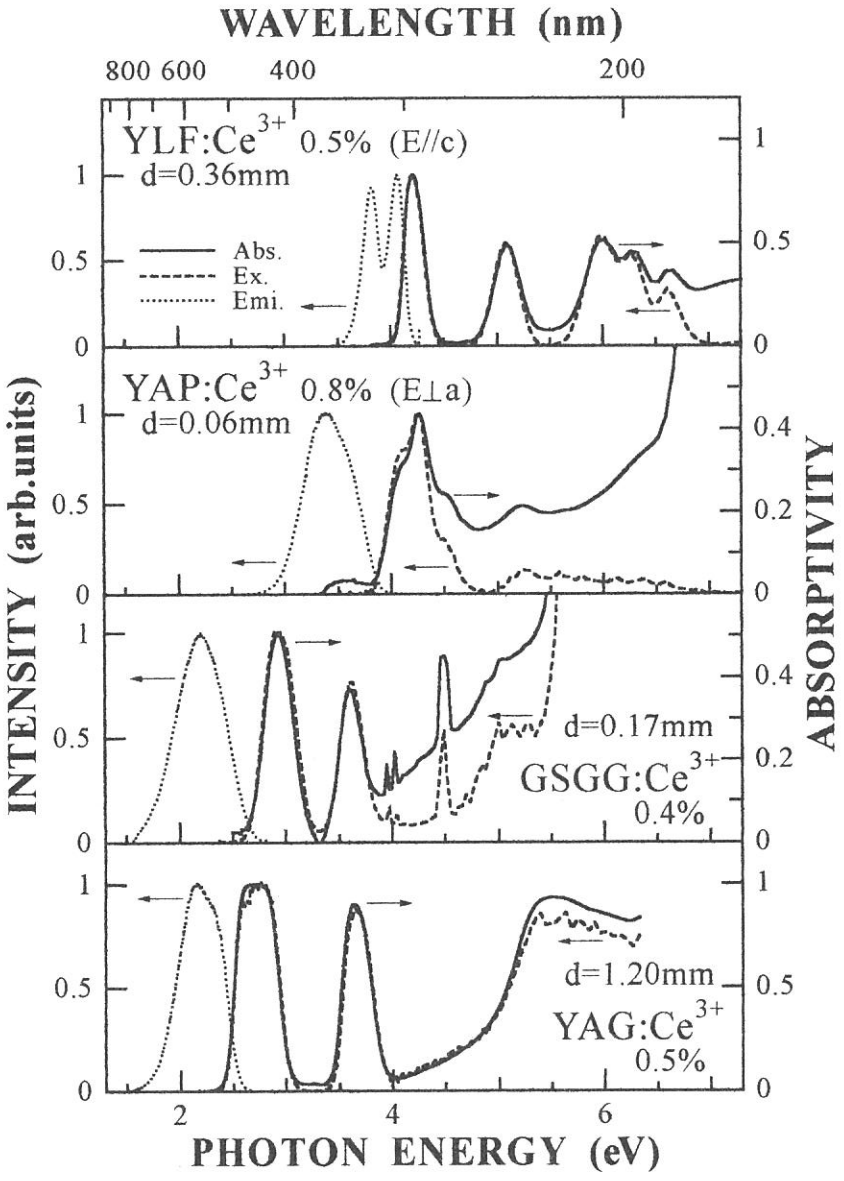

Fig.1 Spectra of Ce doped YAG, GSGG, YAP and YLF at room temperature : absorptivity (solid), emission (dotted) and their excitation spectra (dashed curves) .

References

[1] See, for example, N. Sarukura : Kogaku, **25** (1996) 518 〔in Japanese〕 .

[2] D. S. Hamilton, S. K. Gayen, G. J. Pogatshink, R. D. Ghen, and W. J. Miniscalco : Phys. Rev. **B 39** (1989) 8807.

[3] Y. Suzuki, T. Hirayama, H. Umeta and K. Inoue : this issue.

[4] Li-Ji Lyu and D. S. Hamilton : J.Lumin. **48 & 49** (1991) 251.

[5] C. Pedrini, F. Rogemond and D. S. McClure : J. Appl. Phys. **59** (1986) 1196.

[6] T. Tomiki, F. Fukutome, M. Kaminao, M. Fujisawa, Y. Tanahara and T. Futemma : J. Phys. Soc. Jpn. **58** (1989) 1801.

(BL1B) VUV Excited Luminescence in CsI (pure, Tl-doped and Na-doped) and in multilayer structures of LiF- CaF_2 and LiF- BaF_2.

A. Ejiri, E. Chin, A. Urasaki, T, Yonamine and T. Yokozawa [A]

Dept. of Science Education, College of Education, University of the Ryukyus, Nishihara, Okinawa 903-01.

[A] *Dept. of Physics, Faculty of Science, Rikkyo University, Nishi-Ikebukuro, Tokyo 171.*

CsI is an interesting material of scintillator to be revealed its luminescence mechanism. Alkali earth fluoride crystals (CaF_2 and BaF_2) are well known that they show a strong STE luminescence even at room temperature. [1] It is interesting to investigate quantum confinement effect of the luminescence in the quantum well structures of these fluorides. Samples of scintillators are pure CsI single crystal, Tl- 0. 1mol%- doped CsI and Na- 0. 1mol%- doped CsI crystals.

Present paper will report results of the luminescence measurements in those CsI crystals, and in the quantum well structures respectively consisted of 5- periods of LiF (200Å)- CaF_2 (100Å), LiF (100Å)- CaF_2 (50Å), LiF (200Å)- BaF_2 (100Å), and LiF (100Å)- BaF_2 (50Å). The specimen of 5-periods multilayer structures are fabricated with vacuum evaporation technique and annealing at 200℃ for an hour in every layer after deposition. All measurement were performed at BL-1B by the use of a Spex monochrometer for the luminescence. Excitation spectra for each luminescence band were also measured in the photon energy range up to 40eV. The luminescence spectra were not corrected for the spectral efficiency of the monochrometer and the excitation spectra were normalized by the spectral output of the Seya- Namioka monochromator.

In Fig. 1, observed luminescence spectra in pure CsI and the Tl- doped CsI excited with 12eV radiation at 7K are shown. It is characteristic to be appeared a new band at 2. 5eV in Tl- doped CsI. In Fig. 2, observed luminescence of CaF_2 (exc 1033Å) and BaF_2 (exc 1240Å) single crystals at 7K (a), those of a LiF (200Å)- CaF_2 (100Å) and a LiF (100Å)- CaF_2 (50Å) multilayers at 7K (b), and of a LiF (200Å)- BaF_2 (100Å) and a LiF (100Å)- BaF_2 (50Å) multilayers at 7K (c) are shown.

On the luminescence spectra in the multilayers, several resonance type structures are observed especially on CaF_2 (50Å) spectrum in Fig. 2(b) and BaF_2 (100Å) spectrum in Fig. 2(c). Furthermore, it was found that a line series of luminescence in LiF (200Å)- CaF_2 (100Å) multilayer excited 1050Å at room temperature as shown in Fig. 3(a).

An excitation spectra of the luminescence in the mutilayer structure of LiF(200)-CaF_2 (100) is shown in Fig 3(b). This appears a very narrow band which indicates an onset of STE and a penetration limit of radiation in the multilayer.

The resonance structures and line spectra in the luminescence can be explained in terms of interference of luminescence in the well layers (CaF_2, BaF_2) and of resonant emission in

a cavity of the multilayer.

References

1) A. Ejiri, A. Hatano, and K. Arakaki; UVSOR Act. Rep. (IMS)1995, (1996) 68.

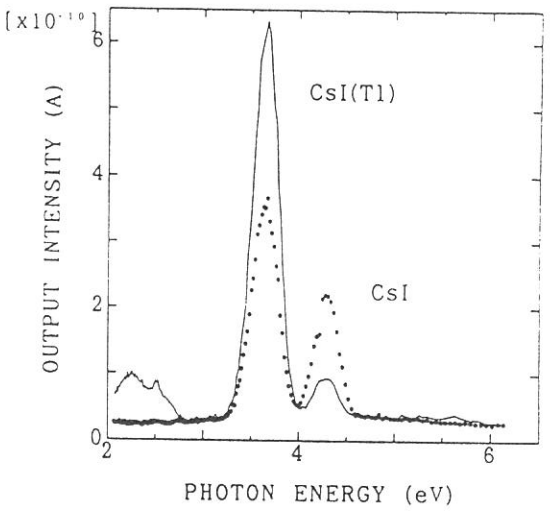

Fig. 1 Luminescence spectra of pure CsI and Tl 0. 1mol%- doped CsI excited with 12eV radiation at 7K.

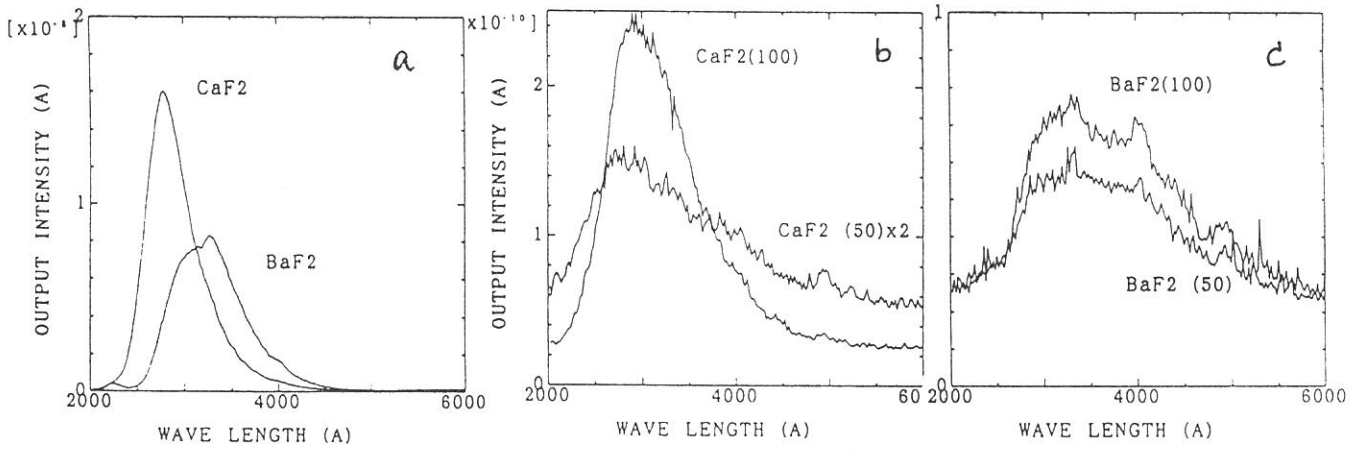

Fig. 2 Luminescence spectra of CaF_2 (excited with 1033 Å) and BaF_2 (excited with 1240Å) crystals at 7K (a), of LiF (200Å)- CaF_2 (100Å) and LiF (100Å)- CaF_2 (50Å) multilayers excited with 1033Å radiation at 7K (b) and of the LiF (200Å)- BaF_2 (100Å) and LiF (100Å)- BaF_2 (50Å) multilayers excited with 1240Å radiation at 7K (c).

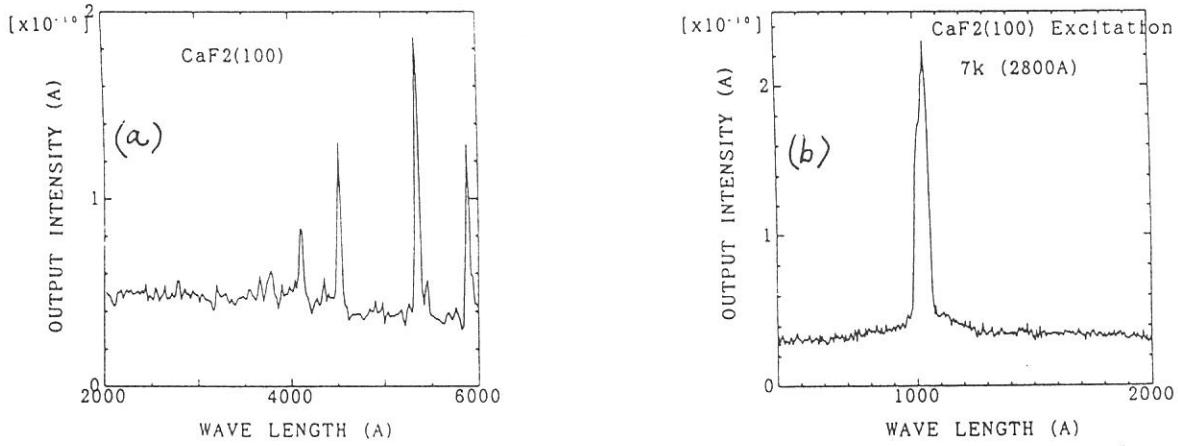

Fig. 3 Luminescence spectra of a LiF (200Å)- CaF_2 (100Å) multilayer excited 1050Å at room temperature(a) and an excitation spectrum of the multilayer luminescence of 2800Å at 7K(b).

(BL1B)

Luminescence from Self-Trapped Excitons in BaFI and $BaFBr_{1-x}I_x$ crystals

Akimasa OHNISHI[A], Ken-ichi KAN'NO[B] and Nobufumi MORI[C]

[A]*Department of Physics, Yamagata University, Yamagata 990-0021*
[B]*Department of Physics, Kyoto University, Kyoto 606-8224*
[C] *Fuji Photo Film Co., Ltd., Miyanodai, Kaisei-machi, Kanagawa 258-0023*

Balium-fluoro-halides (BaFX, X=Cl, Br, I) are important host materials of photo-stimulated luminescence phosphors activated with Eu^{2+} ions.[1] We have investigated luminescence properties from self-trapped excitons (STEs) in BaFCl, BaFBr and $BaFCl_{1-x}Br_x$, and have discussed on the STE configurations by the analogy with on- and off-center STEs in alkali halides.[2,3] In the present study, luminescence measurements have been extended to BaFI and $BaFBr_{1-x}I_x$ crystals.

BaFI and $BaFBr_{1-x}I_x$ were grown by a horizontal Bridgmann method. Experiments were made using synchrotron radiation pulses from the beam line BL1B of UVSOR. Luminescence was detected with a photomultiplier (Hamamatsu R955) through a grating monochromator (Spex 270M).

Figure 1(a) shows the emission spectrum in BaFI at 15 K. When the crystal is excited at 8.86 eV in the range of band-to-band transition, a characteristic luminescence band is observed at 4.54 eV. In Fig.1(b), is shown the excitation spectrum for the 4.54 eV band, along with positions of the halogen doublet due to I^- spin-orbit splitting reported by Nicklaus [4] (arrows at 6.5 and 7.6 eV). The spectrum indicates high emission yields above the threshold at 6.5 eV. This suggests that the 4.54 eV band is due to recombination luminescence from STE with I_2^--core in BaFI. Efficient excitation bands are observed also in the region (5.6 ~ 6.5 eV) of low energy tail of the n=1 exciton absorption band. The reason is now under consideration.

To see the effect of changing in the crystal environment on the manner of exciton self-trapping, luminescence from $BaFBr_{1-x}I_x$ has been investigated under excitation at 10.3 eV at 10 K. Their emission spectra are shown in Fig.2. As seen in Fig.2(a), an emission band is observed at 5.06 eV in the x=0.001 crystal, as far as the excitation is made at the energies of band-to-band transition of BaFBr. The peak energy and band width are in good agreement with the intrinsic luminescence band of BaFBr. This means that the STE composed of an electron and a Br_2^- core is created under excitation at 10.3 eV. However when excited at the lower energy around 6.53 eV, another emission band which can be attributed to the localized excitons with $(BrI)^-$-cores appears at 5.18 eV (dotted spectrum of Fig.2(a)). In the case of x=0.1, a new emission band is observed at 4.95 eV together with the 5.18 eV band. In this case, major part of free holes must be self-trapped on I^- sites because of the smaller electron affinity of I^- compared with Br^-. Thus the 4.95 eV band supposedly originates from the localized excitons with I_2^--cores. In fact, the 5.18 eV band disappears in the x>0.3 crystals, and the 4.95 eV band gradually

shifts to the low energy side with the increase in x and finally connects to the 4.54 eV band from the STE with I_2^--core in BaFI. It should be noted that these spectral changes in $BaFBr_{1-x}I_x$ are essentially the same as those of on-center type STE luminescence in $BaFCl_{1-x}Br_x$.[3] We suppose that the STE configurations responsible for the emission bands are also of on-center type, and the off-center instability does not take place in BaFI and $BaFBr_{1-x}I_x$.

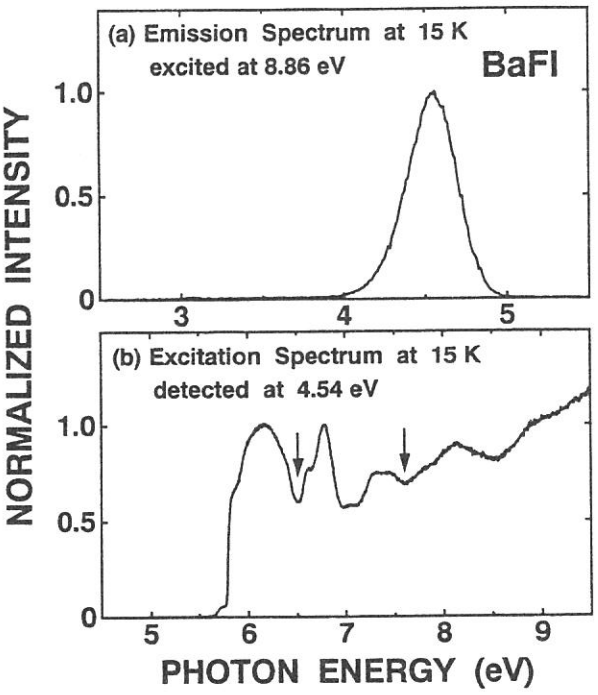

Fig.1

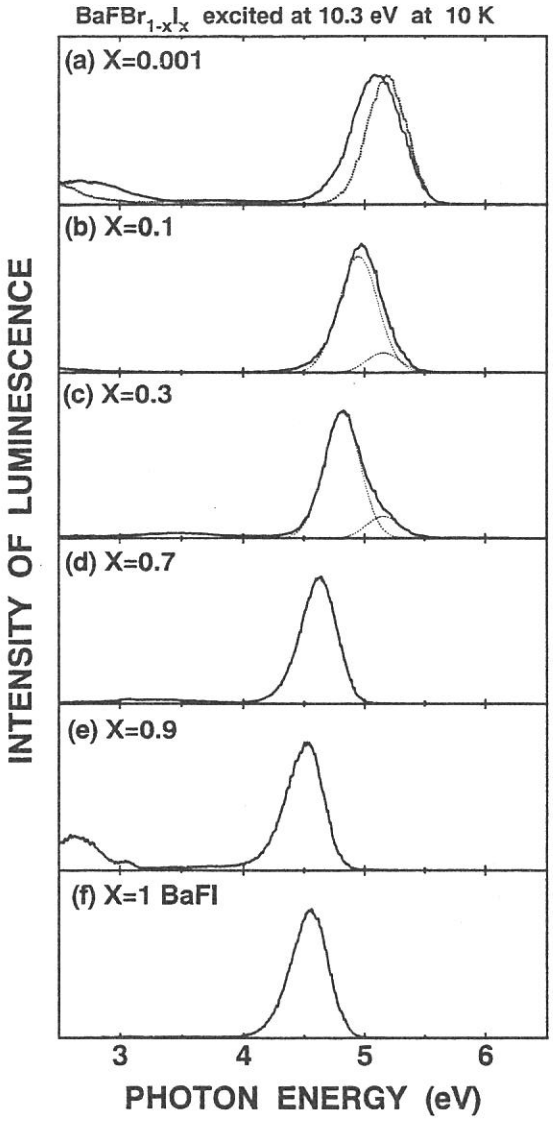

Fig.2

References

1. M. Sonoda, M. Takano, J. Miyahara and H. Kato ; Radiology, 148 (1983) 833.
2. A. Ohnishi, K. Kan'no, Y. Iwabuchi and N. Mori ; Nucl. Instr. and Meth. in Phys. Res. B91 (1994), 210.
3. A. Ohnishi, K. Kan'no, Y. Iwabuchi and N. Mori ; J. Electron Spectrosc. Relat. Phenom., 79 (1996) 163.
4. Nicklaus ; Phys. Status. Solidi (a) 53 (1979) 217

(BL1B)

Optical Spectra in Solid Superoxide KO_2

M. ASHIDA, O. MORIKAWA, S. HASHIMOTO[A], S. HIROSE[B], M. KAMADA[B] and K. KAN'NO

Department of Physics, Kyoto University, Kyoto 606

[A]Kyoto University of Education, Kyoto 612

[B]UVSOR, Institute for Molecular Science, Okazaki 444

Alkali superoxides consist of alkali metal ions and paramagnetic anion O_2^- molecules. This material shows a number of structural phase transitions due to the reorientation of O_2^- [1] and antiferromagnetic order of the spin 1/2 of O_2^-. [2] The O_2^- molecule in alkali halides is a well-known efficient luminescent center.[3] Thus characteristic optical properties reflecting the phase transition are expected in the alkali superoxides. However, there have been only a few optical studies on solid alkali superoxides, since they are highly reactive and it is difficult to obtain single crystals of appropriate size. Bösch *et al.* succeeded in growing single crystals of NaO_2 in liquid ammonia and measured reflection spectra.[4] For the other alkali superoxides, optical spectra in visible and VUV region have not been reported yet. As a first step for the study of optical properties of this system, solid KO_2 was investigated in the present experiment. Samples were prepared by cooling molten KO_2 on Al substrates in a vacuum.

Reflection spectra in KO_2 at 40K and 310K are shown in Fig. 1. The overall structure and peak positions of the spectra were reproducible, though the absolute value of the reflectivity changed within ±10% from sample to sample. It is regrettable that the spectra in the low energy region below ~4eV, where anomalous temperature change was observed in NaO_2 crystal,[4] were affected by the back reflection due to the Al substrate. Although the spectrum changed gradually with increasing temperature, characteristic changes at the phase-transition temperatures were not observed. The structures below ~7eV (e.g. the remarkable peak at 6eV) correspond to those in NaO_2 crystal.[4] Hence, the spectral features in the lower energy region (4-7eV) can be assigned to the intramolecular transition in the O_2^- molecule and those in the higher energy region are possibly caused by the charge transfer transition. The structures due to the intramolecular transition, however, cannot be explained by using the adiabatic potential diagram of a single molecule.[5] The transition $^2\Pi_g \rightarrow {}^2\Pi_u$ of an O_2^- molecule, which gives rise to a main absorption band centered at ~5eV of O_2^- centers in alkali halides,[6] does not manifest itself in Fig. 1. The effect of the interaction among the O_2^- molecules, that is, Frenkel exciton, and/or the electron-phonon interaction must be taken into account.

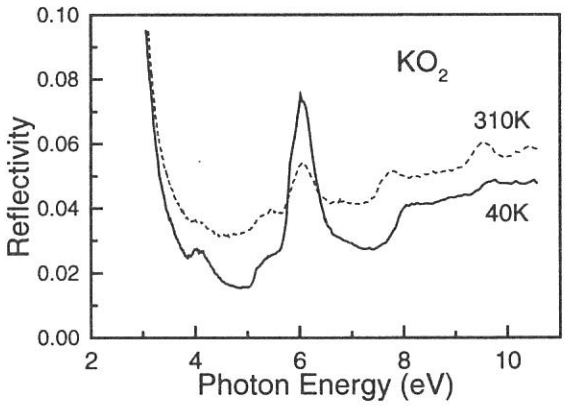

Fig. 1. Reflection spectra in solid KO_2. (Solid line: 40K, broken line: 310K.)

Photo-luminescence was observed even at room temperature. Figure 2 shows its spectrum at 310K under the excitation at ~6eV. The broad shape almost unchanged down to ~10K. The excitation spectrum of this luminescence is shown in Fig. 3. The remarkable peaks and a shoulder are in good agreement between excitation and reflection spectra. Therefore, it is confirmed that the luminescence arises from the intrinsic excited state of KO_2. The luminescence spectrum is drastically different from the spectra of O_2^- centers in alkali halides, which show sharp vibronic lines.[3] This fact indicates strong intermolecular interaction among O_2^- molecules and/or electron-phonon interaction in alkali superoxides again. For further investigation, growth of single crystals of alkali superoxides is desirable.

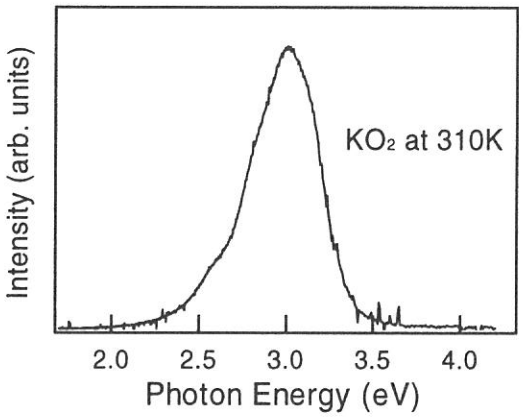

Fig. 2. Emission spectrum in KO_2 at 310K under excitation at 205nm.

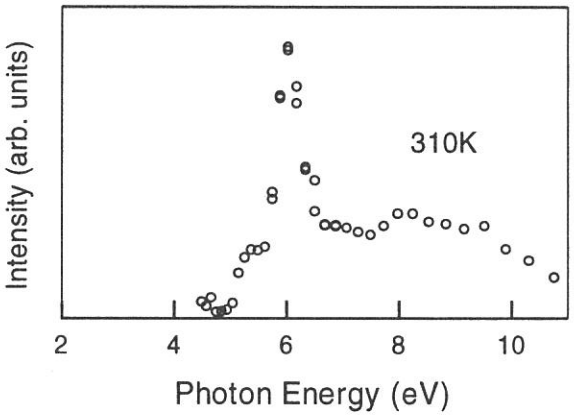

Fig. 3. Excitation spectrum of 3.0eV emission in KO_2 at 310K.

References

1) M. Ziegler *et al.*: Helv. Phys. Acta **49** (1976) 57.
2) H. G. Smith *et al.*: J. Appl. Phys. **37** (1966) 1047.
3) S. Hongo *et al.*: Memoirs of the Faculty of Science, Kyoto University, A **38** (1992)187.
4) von M. Bösch and W. Känzig: Helv. Phys. Acta **48** (1975) 743.
5) M. Krauss *et al.*: Phys. Rev. **A7** (1973) 69.
6) F. Fischer *et al.*: Z. Phys. **189** (1966)79.

(BL1B)

Reflection Spectra of Orthorhombic and Cubic PbF_2 Crystals

Masami FUJITA, Dmitri L. ALOV,[A] Minoru ITOH,[B] Jun-ichi MURAKAMI,[B]
Tetsuo SAIDA,[C] Hideyuki NAKAGAWA[C] and Mamoru KITAURA[D]

Maritime Safety Academy, Wakaba, Kure, Hiroshima 737-8512
[A]*Institute of Solid State Physics, Chernogolovka, Moscow, 142432, Russia*
[B]*Department of Electrical and Electronic Engineering, Faculty of Engineering, Shinshu University, Wakasato, Nagano 380-0922*
[C]*Department of Electrical and Electronics Engineering, Faculty of Engineering, Fukui University, Bunkyo, Fukui, 910-0017*
[D]*Fukui National College of Technology, Sabae, Fukui, 916-0064*

Lead fluoride crystallizes into two phases, one of which has an orthorhombic lattice of $PbCl_2$ type (α-PbF_2: D_{2h}^{16}, Pmnb) and the other has a cubic fluorite structure (β- PbF_2: O_h^5, Fm3m). The former is more stable phase below 320 °C, but the latter is also metastable at low temperature. Optical spectrum of β- PbF_2 reported so far[1] shows different features from the orthorhombic $PbCl_2$ and $PbBr_2$[2]. It is an interesting problem whether the difference in optical spectra comes from the difference in the crystal structure or in the halogen species. However, optical study of PbF_2 has been limited so far to the cubic phase because of the difficulty in preparing the orthorhombic crystals with enough size. Recently, orthorhombic crystals have been grown from aqueous solution and the photoluminescence experiment has been performed[3,4]. In the present study, reflection spectra of α-PbF_2 have been measured up to VUV region in order to investigate the electronic structure in lead halides.

Single crystals of α-PbF_2 were grown from the aqueous solution as thin flakes with the size of 2 x 2 mm^2. The surface of the sample was perpendicular to the c-axis. Reflection spectra were measured for the polarization parallel to the a-axis (E//a) or b-axis (E//b). Reflection spectra of cleaved surfaces of β-PbF_2 crystal and PbClBr crystal were also measured. Experiments have been performed at BL1B in UVSOR.

In the upper part of Fig. 1 are shown reflection spectra of α- and β-PbF_2 crystals at 7K. In the spectra of α-PbF_2, the first exciton band 1 appears at 5.7eV. As mentioned later, the band shows dichroism. Two prominent peaks 2 and 3 are found at 6.3 eV and 8.5 eV. These structures above 6 eV depend slightly on the polarization. The spectrum of β-PbF_2 agrees with that measured at 77K[1]. The first exciton band of β-PbF_2 appears nearly the same position of the exciton band of α-PbF_2. In the 6-7 eV region is observed a broad band 2 which seems to consist of two or three components. A large peak 3 is observed at 8.6 eV. Gross features in the spectra of α-PbF_2 resemble those of β-PbF_2, which suggests that the electronic structures in both modifications are similar to each other.

Reflection spectra in the first exciton band region of α-PbF_2 are shown in Fig. 2. The second-energy-derivative reflectance d^2R/dE^2 (2EDR) spectra were calculated numerically from the reflection spectra and are also shown in Fig. 2. The 2EDR spectra clearly indicate that the exciton band has a single peak for E//a, while it consists of two components for E//b. The peak positions determined from the 2EDR spectra are, 5.678eV (1a) for E//a, and 5.701eV (1b) and 5.829eV (1b') for E//b. The first exciton band of $PbCl_2$ and $PbBr_2$ shows similar dichroism, that is, the band has one peak for E//a and two peaks with separation of 60meV for E//b[2]. The dichroism is explained in terms of the cationic $6s^2 \rightarrow 6s6p$ ($^1S_0 \rightarrow {}^3P_1$) transition in the crystal field of Cs symmetry around the lead ion. According to the theoretical

calculation based on the point charge model, the crystal field splitting of the $6p$ levels in α-PbF_2 is about two times larger than that in $PbCl_2$ and $PbBr_2$[5]. This is in agreement with the present experimental result.

In the lower part of Fig. 1 are shown reflection spectra of $PbCl_2$, PbClBr and $PbBr_2$ at low temperature. The sharp peaks 1 and 3 in these crystals shift continuously with the change of halogen component. This indicates that the excitation associated with the peak 3 occurs also mainly at the cation site. The energy position of the peak 3 of $PbCl_2$ and $PbBr_2$ almost coincides with the C-absorption band of Pb^{2+} impurity in alkali chloride and bromide, respectively. Therefore the peak 3 of these crystals is considered to be due to the excitonic transition corresponding to the $^1S_0 \rightarrow {}^1P_1$ excitation in lead ions[2]. In PbF_2, the transition is expected to occur in the 7.5-8.0 eV region from the extrapolation of $PbBr_2$ and $PbCl_2$ indicated by the broken line in Fig. 1. However, no sharp structure is discernible at the position in the spectra of PbF_2. The peak 3 at 8.5 eV is too broad to be assigned to such transition. Present result indicates that the transition intensity corresponding to the $^1P_1$ excitation is strongly affected by the halogen species, in spite of the localized nature of the cationic excitation. The question why the transition does not appear in PbF_2 would be an important problem to understand the electronic structure in lead halides.

References

[1] J. H. Beaumont, A. J. Bourdillon and J. Bordas: J. Phys. C Solid State Phys. **10**(1977)761.

[2]M. Fujita, H. Nakagawa, K. Fukui, H. Matsumoto, T. Miyanaga and M. Watanabe: J. Phys. Soc. Jpn. **60**(1991)4393.

[3]A. B. Kulakov, A. A. Zhokhov, G. A. Emel'chenko and N. V. Klassen: J. Cryst. Growth **151**(1995)107.

[4]D. L. Alov and S. I. Rybchenko: J. Phys. Condens. Matter 7(1995)1475.

[5]K. Wada: Sci. Light **26**(1977)77.

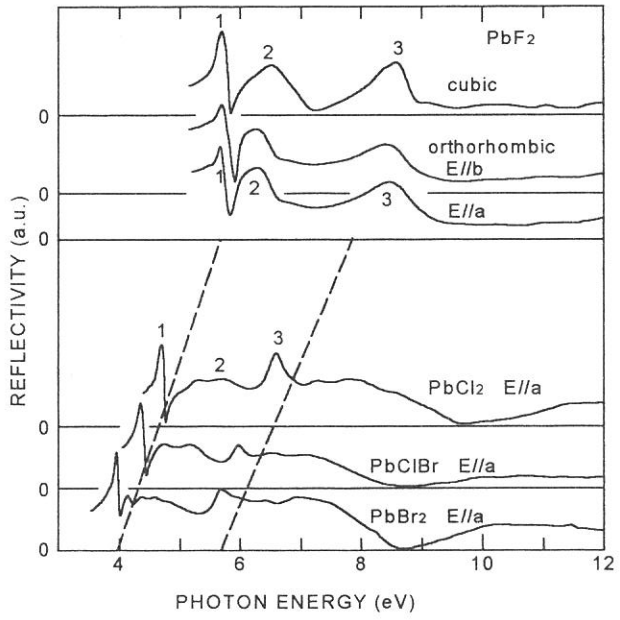

Fig. 1. Reflection spectra of lead halides at low temperature.

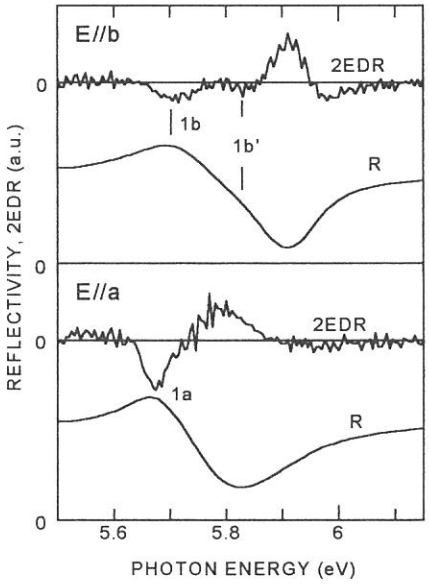

Fig. 2. Reflection and 2EDR spectra of α-PbF_2 in the first exciton band region.

(BL1B)

Time-Resolved Luminescence from Excitons Localized at Br^- Impurities in CsCl Crystals

Y. Bokumoto, M. Itoh and H. Yoshida*

Faculty of Engineering, Shinshu University, Nagano 380-8553
**NEC Kansai, Ltd., Shiga 520-8555*

In CsCl crystals containing a small amount of Br^- impurities, three luminescence bands can be seen at 3.84, 4.35 and 5.27 eV under the excitation with UV light in the low-energy region of the fundamental absorption of host CsCl [1]. It has been suggested that the 3.84-eV band is due to radiative decay of off-centered excitons localized at Br^- impurity monomer. The 4.35- and 5.27-eV bands are likely due to off- and on-centered excitons localized at Br^- impurity dimer, respectively. In the present work, we have carried out time-resolved luminescence studies on localized excitons in CsCl:Br, in order to investigate relaxation processes of the excitons in CsCl crystals with simple cubic structure.

Figure 1 shows time-resolved luminescence spectrum of $CsCl_{1-x}Br_x$ (x = 0.005) excited with 7.56-eV light under the single-bunch operation of synchrotron radiation (SR) at 10 K. Broken curve (fast component) and solid curve (slow component) represent the counts of photons measured through the time window of 0 − 2.4 ns and 37 − 60 ns after the excitation pulse, respectively. The 3.84-eV band does not change its peak position in both spectra. On the other hand, the peak position of the 4.35-eV band shifts from 4.60 eV in the fast-component spectrum to 4.35 eV in the slow-component spectrum. From Fig. 1, it is clear that the 5.27-eV band has only fast decay component (decay time = 0.55 ns).

Decay profile of the luminescence detected at 4.35 eV, i.e., the peak position of the slow-component spectrum in Fig. 1, is shown by dotted curve in Fig. 2, where the slow decay component has been subtracted. Open circles represent the pulse shape of SR. As clearly seen, this decay profile has a rise component around 1 ns.

Luminescence spectra have also been examined in the temperature ranges from 8.3 K to 200 K under stationary UV-light excitation. It is found that the 4.35-eV band exhibits remarkable blue-shift toward 4.6 eV with increasing temperature from 8.3 K up to 40 K.

All the above results suggest that there are two excited states on the pathway of the off-center relaxation of excitons localized at Br^- dimer in CsCl system; one is a stable state responsible for the 4.35-eV luminescence, and the other is a metastable state for the 4.60-eV luminescence. At low temperatures, the localized excitons first relax to the metastable state, from which the 4.60-eV photons are emitted. A part of them are then converted to the stable state over a potential barrier, resulting in the 4.35-eV luminescence. If the temperature is increased above 40 K, the relaxed excitons are repopulated at the 4.60-eV state. According to this model, decay profile of the

luminescence detected at 4.35 eV can be expressed by the formula;

$$I(t)=\int_0^{\infty} G(\xi)\cdot\left\{W_{f1}\,e^{-(W_{f1}+W_T)(t-\xi)}+C\cdot W_{f2}\left(\frac{W_T}{W_{f1}+W_T-W_{f2}}e^{-W_{f2}(t-\xi)}-\frac{W_T}{W_{f1}+W_T-W_{f2}}e^{-(W_{f1}+W_T)(t-\xi)}\right)\right\}d\xi, \quad (1)$$

where W_{f1} and W_{f2} are the radiative transition probabilities of the 4.60- and the 4.35-eV states, respectively, and W_T is the transition rate from the 4.60-eV state to the 4.35-eV state. $G(\xi)$ is the pulse shape of SR and C is a constant which includes the ratio of the luminescence yields of the 4.60- and 4.35-eV bands. The slow decay process of the 4.35-eV state is neglected in Eq. (1). From this fit we get $1/W_{f1}$ = 1.3 ns, $1/W_{f2}$ = 3.0 ns, $1/W_T$ = 1.3 ns and C = 5. Agreement between the calculated and experimental curves seems fairly good.

The present experiment reveals that the off-centered excitons localized at Br^- dimer have two different relaxed-configurations; stable and metastable ones. This situation is somewhat different from that in alkali-halide crystals with NaCl-type structure [2].

The authors are grateful to Professor K. Sawada for useful discussion.

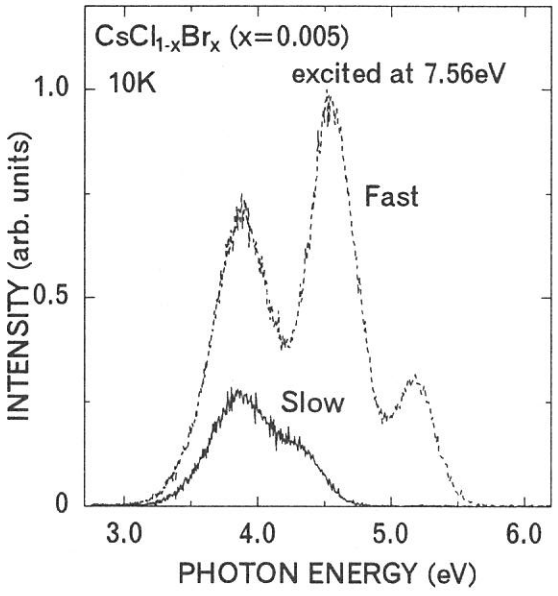

Fig.1. Time-resolved luminescence spectrum excited with 7.56-eV photons at 10K.

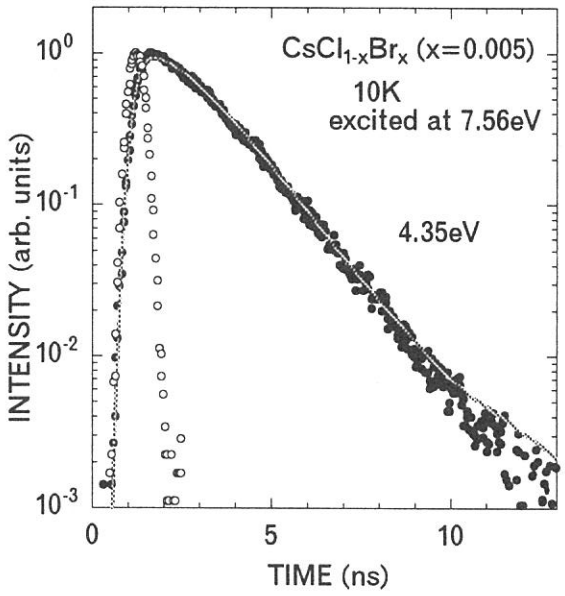

Fig.2. Decay curve (closed circles) of the luminescence detected at 4.35 eV under the excitation with 7.56-eV photon pulses at 10 K. Open circles represent the pulse shape of SR. Solid curve is the best fit of Eq. (1).

[1] H. Yoshida, N. Ohno and M. Itoh; *Proc. 2nd Int. Conf. on Excitonic Processes in Condensed Matter*, Kurort Gohrisch, edited by M. Schreiber (August, 1996) p.231.

[2] K. Kan'no, K. Tanaka and T. Hayashi; Rev. Solid State Sci. 4 (1990) 383.

(BL1B)

Two-Photon Spectroscopy of Excitons in BaF_2 by Combinational Use of Synchrotron Radiation and Laser

O. Arimoto[a], T. Tsujibayashi[b], M. Watanabe[c], S. Fujiwara[a], M. Itoh[d], S. Nakanishi[e], H. Itoh[e], S. Asaka[f], and M. Kamada[g]

[a]*Department of Physics, Okayama University, Okayama 700-8530*
[b]*Department of Physics, Osaka Dental University, Hirakata 573-1121*
[c]*Department of Fundamental Sciences, Kyoto University, Kyoto 606-8501*
[d]*Department of Electrical & Electronic Engineering, Shinshu University, Nagano 380-8553*
[e]*Department of Advanced Materials Science, Kagawa University, Takamatsu 760-8526*
[f]*Equipment Development Center, Institute for Molecular Science, Okazaki 444-8585*
[g]*UVSOR Facility, Institute for Molecular Science, Okazaki 444-8585*

One-photon spectroscopy with synchrotron radiation (SR) is a powerful and useful tool for the studies of electronic structures of various materials over a wide spectral range. On the other hand, laser has been utilized for not only one-photon spectroscopy but also multi-photon spectroscopy because of its high power and narrow spectral width. Combinational use of these two light sources is interesting and promising for the spectroscopy of solids in the VUV region. In the present study we have carried out a two-photon spectroscopy of the excitons in BaF_2 by making use of SR and laser. The valence band of BaF_2 consists of $2p$ orbital of F^-, and the conduction band $6s$ and $5d$ orbitals of Ba^{2+}. Therefore the excitons with an envelope function of S-type are one-photon allowed while the P excitons are two-photon allowed. A preliminary result at room temperature has been already reported [1, 2]. In this work, the experimental system has been improved to obtain definite results at low temperatures.

The experiments were done at BL1B of UVSOR. In Fig. 1 is shown a schematic diagram of the apparatus used for the present work. Single crystals of BaF_2 were cleaved from the ingot and mounted on a cold finger of a conduction-type cryostat. The monochromatized SR light (pulse width ~ 400 ps) was introduced into a sample chamber along the opposite direction of the second harmonic light of a Nd:YAG laser (2.33 eV, pulse width ~ 70 ns, average power ~ 12 W). The RF signal of 90 MHz from the master oscillator of the electron storage ring was divided down to 5 kHz, which triggers the YAG laser. The time interval between successive SR pulses was about 11 ns, while the time width of the laser pulse was 70 ns. Therefore, the time coincidence between the SR and laser pulses was automatically achieved, because about six pulses of the SR were involved within the time duration of a single pulse of the laser. This is an advantageous point compared to the preliminary experimental system with a short-pulse laser [1, 2], in which the temporal coincidence between the SR and laser pulses had to be carefully adjusted. Furthermore, the use of the high-repetition laser with the wide pulse-duration and low peak-power enabled us to detect weak two-photon signals more efficiently without any damage of the sample. The luminescence at about 4.1 eV, which is due to self-trapped excitons (STE's) produced by two-photon excitation, was observed by a micro-channel plate photomultiplier tube (MCP-PMT), with a combination of filters and a conventional monochromator for eliminating the scattered light from the laser. The signals from the MCP-PMT were fed to a three-channel time-gated photon counter. The photon signals just before and after the incidence of the laser pulses were counted at the channels 1 and 2, respectively: The channel 1 (CH 1) counts the background signal induced only by the SR light, while the CH 2 counts the signal due to the STE luminescence induced by the simultaneous irradiation with the SR and laser lights in addition to the background signal. The gate widths for both counters were equally set to be 4 μs by referring to the lifetime of the STE luminescence. The total signal was also counted at the CH 3 with the time-gate in full

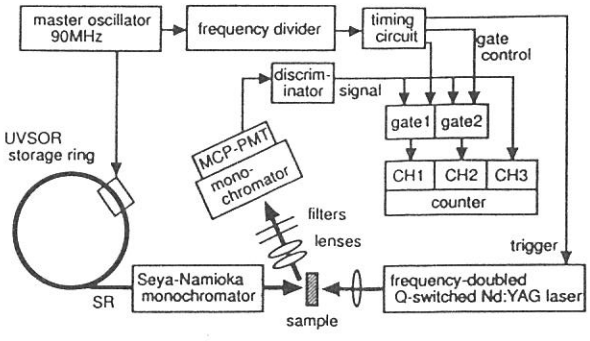

Fig. 1 Schematic diagram of the experimental system for two-photon spectroscopy with SR and laser.

open. The net luminescence signal induced by two-photon excitation was obtained by subtracting the count at CH 1 from that at CH 2. The above detection system has been specially developed for the present experiments, the details of which will be reported elsewhere [3].

Open circles in Fig. 2 show two-photon excitation spectrum of BaF_2 measured by monitoring the STE luminescence at 15 K. Its intensity corresponds to the net luminescence count obtained by subtraction of the count at CH 1 from that at CH 2. The solid curve is the total count at CH 3, which is properly normalized around 10 eV to the two-photon spectrum shown by the open circles. The closed circles are obtained by subtracting the data shown by the solid curve from those by the open circles. The count due to the net two-photon process, which is the difference between the count at CH 1 and that at CH 2, was at most 1% of that at CH 3. Accordingly the solid curve, intensity of which is proportional to the total count at CH 3, can be regarded as the one-photon spectrum induced by the SR light alone. As is easily recognized in the figure, the two-photon spectrum shown by open circles resemble the one-photon spectrum shown by solid curve. Such a similarity invokes the existence of cascade processes: Real states (or their relaxed states) excited by one photon from the SR are subsequently re-excited to the higher states by the laser, which in turn contributes to the enhancement of the STE luminescence. This is in contrast to the usual two-photon absorption process, in which virtual intermediate states are involved. In the one-photon excitation spectrum of the STE luminescence we observed weak peaks at 8.3 eV and 8.8 eV probably due to excitons bound to some unknown lattice imperfection. The energy positions of the two peaks at 10.6 eV and 11.2 eV in Fig. 2 are in good correspondence to those of the weak peaks at 8.3 eV and 8.8 eV. Therefore it is likely that the real excited states are unknown bound exciton states. Here it is noted that we made careful checks about not only the reproducibility of data but also the instruments used, especially the time-gated counter, to make sure that the obtained experimental data are reliable enough.

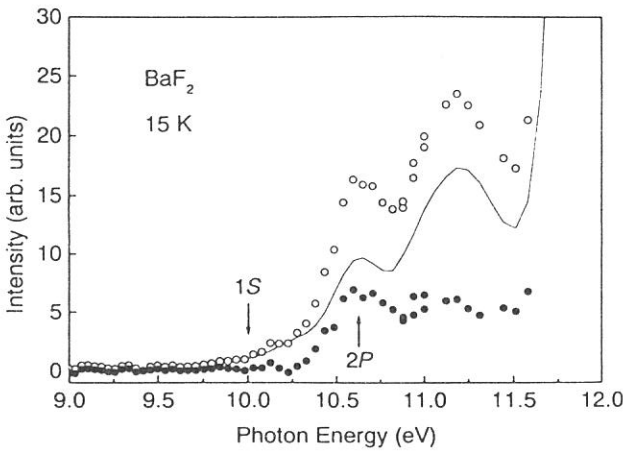

Fig. 2 The two-photon excitation spectrum of the STE luminescence in BaF_2 at 15 K (open circles). The spectrum includes two contributions: the two-photon absorption process (closed circles) and the cascade excitation process (solid curve).

As mentioned above, closed circles in Fig. 2 are the result of subtraction of the spectrum shown by the solid curve from that by the open circles. Since the former refers to the count due to the cascade process and the latter the net count due to the two-photon processes, the resultant spectrum depicted by closed circles can be regarded as the spectrum due to the usual two-photon absorption process under the assumption that the efficiency of the cascade excitation is constant. The spectrum has a broad band peaking at 10.6 eV. This is 0.6 eV higher than the 1*S* exciton whose energy position is indicated by a downward arrow. We assign this peak to the 2*P* exciton. Assuming a simple hydrogen model, the binding energy of the 1*S* exciton is estimated to be 0.8 eV, which gives the band gap energy as 10.8 eV. From measurements of reflection spectra, Rubloff has deduced the band gap energy of 11.0 eV [4], whereas Tomiki and Miyata have obtained the value of 10.6 eV [5]. It seems that the present value of 10.8 eV is more accurate because we observed the definite peak of the 2*P* exciton. Finally it is to be stressed that cascade excitation processes like the present case are not yet easy to investigate by the use of usual lasers, since their one-photon energies fall into the transparent region of the materials with wide band gap so that the real excited states can not be excited.

References

[1] T. Tsujibayashi *et al.*: UVSOR Activity Report **24** (1997) 52.
[2] M. Kamada *et al.*: *Proc. 6th Int. Conf. Synchrotron Radiation Instrum.*, Himeji, Aug. 1997 (in press).
[3] S. Asaka *et al.*: submitted to Rev. Sci. Instrum.
[4] G. W. Rubloff: Phys. Rev. **B5** (1972) 662.
[5] T. Tomiki and T. Miyata: J. Phys. Soc. Jpn. **27** (1969) 658.

(BL3A1)

Total Photoyield in Amorphous Chalcogenide Films by Undulator Radiation

Koji HAYASHI

Center for Cooperative Research, Gifu University, Gifu 501-1193

It is well-known that amorphous materials show a variety of photoinduced phenomena. The prominent photoinduced phenomenon in these materials is a time-dependent decrease in photocurrent during and after bandgap illumination.[1,2] This phenomenon is usually called photodegradation and is explained in terms of light-induced metastable defects (LIMD). In the device application of these materials, LIMD creation is a serious problem. Although a number of models have been proposed for LIMD creation[3], details of the mechanism underlying LIMD creation in these materials are still not clear. Understanding the physical mechanism underlying metastability is one of the important fundamental problems related to these materials. These phenomena were studied by exciting outer core electrons with the irradiation of the bandgap illumination. Little attention has been given to the photoinduced phenomena by exciting inner core electrons with the irradiation of higher energy photon. To obtain a wide knowledge of the photoinduced effects, it is necessary to investigate photoinduced effects on wide energy range. In the previous reports[4], we have reported the photodarkening in amorphous arsenic trisulfide (a-As_2S_3) by the vacuum ultra-violet (VUV) light. In the present study, we performed an in-situ study of the photoinduced effects by exciting inner core electrons and observed photoinduced change in total photoyield during illumination of the VUV light.

Thin films of a-As_2S_3 used for the measurements of photoyield were prepared onto quartz substrates by conventional evaporation technique. The thickness of the films was around 6000Å. An electrode using Al contact was fabricated first on the substrate for the measurements of the photoyield, before depositing the amorphous films. The experiments were performed at a BL3A1 beam line of the UVSOR facility of the Institute for Molecular Science in Okazaki. VUV light that is filtered through an Al film from undulator radiation was used to measure the photoyield. Before illumination, the samples were annealed at 443K (near the glass transition temperature) for two hours in a vacuum. To eliminate visible lights of synchrotron radiation and higher harmonics of undulator radiation, Al film was inserted between undulator and samples. The samples were fixed in sample chamber which were evacuated below 10^{-8} Torr. The photon flux of undulator radiation through Al film was estimated from the total photoelectric yield of gold mesh.

Figure 1 shows the change in the total photoyield as a function of number of photons for a-As_2S_3 at room temperature. This figure is obtained by normalizing the photoyield to the incident photon flux. As shown in the figure, the photoyield is decreased at the first stage. At the second stage, the photoyield is gradually increased and the photoyield seems to be finally saturated. This change also depends on the illumination energy of the photon. This change is similar effects with the previous report[5] in the photocurrent by VUV light. That is, the decrease and the increase in the photoyield are related with the LIMD creation (or initial defects) and photodarkening , respectively.

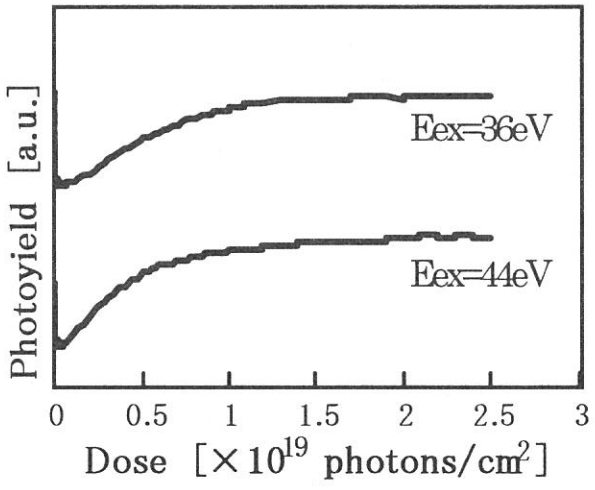

Fig.1 Change in the total photoyield for a-As_2S_3 measured at room temperature.

REFFERENCES

[1] K. Shimakawa, S. Inami, and S. R. Elliott, Phys. Rev. B, 42(1990)11857.
[2] D. L. Staebler and C. R. Wronski, Appl. Phys. Lett., 31(1977)292.
[3] K. Shimakawa, A. Kolobov, and S.R. Elliott, Adv. Phys., 44(1995)475.
[4] K. Hayashi, D. Kato, and K. Shimakawa, J. Non-Cryst. Solids., 198-200(1996)696.
[5] K. Hayashi, A. Hirai and K. Shimakawa, UVSOR Activity Report 1996, p116.

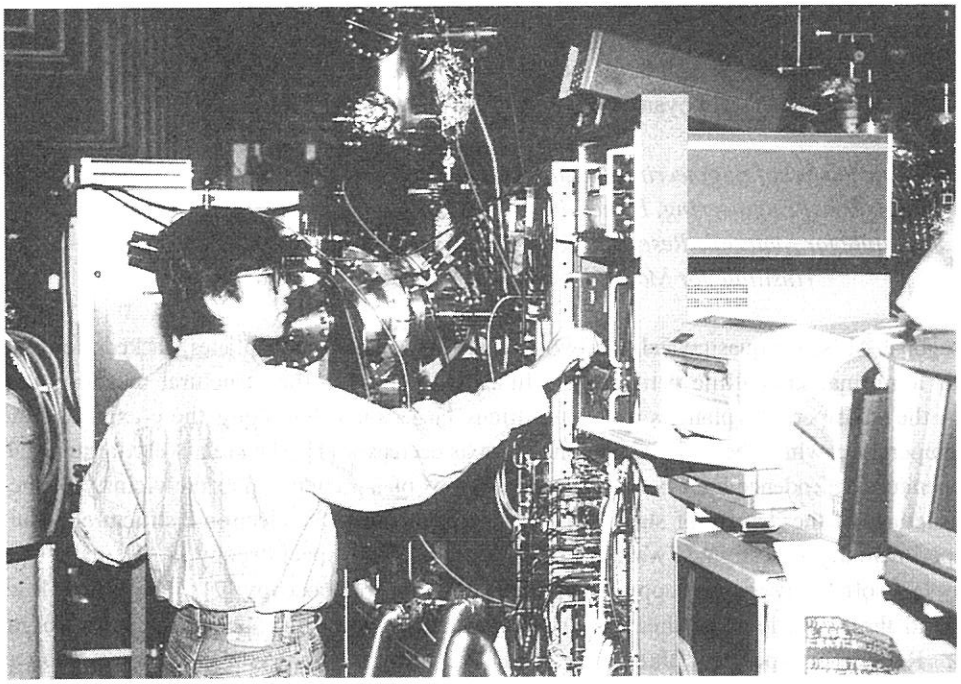

BL8B1

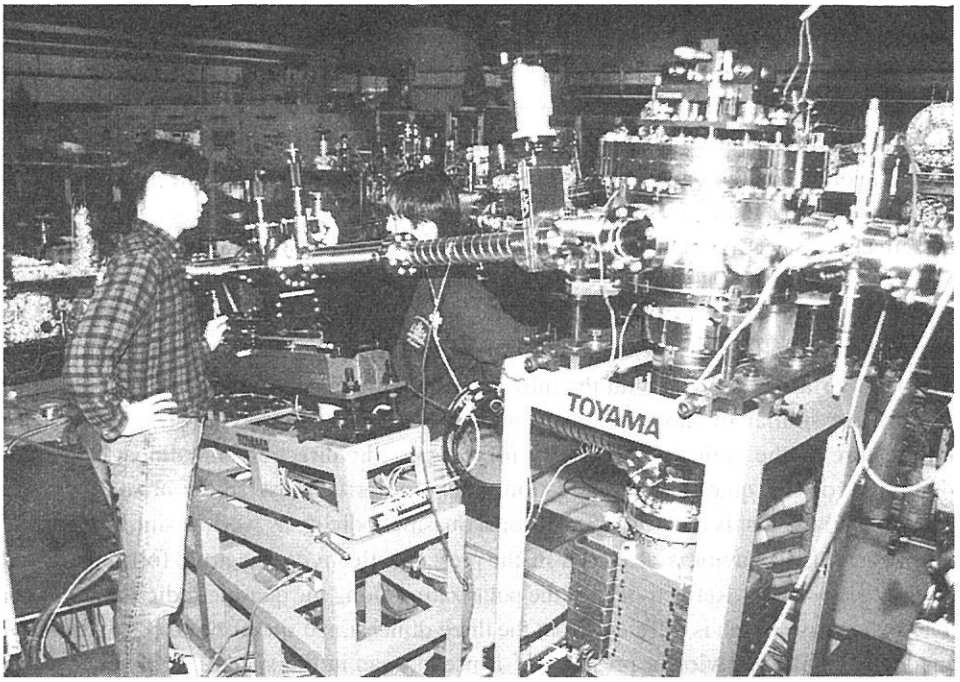

BL2B2

(BL6A1)

Infrared Reflectivity Spectra of Decagonal Al-Ni-Co Single Crystal

K. Soda, Y. Yanagida, K. Nozawa, T. Takeuchi, K. Morita, U. Mizutani,
Y. Yokoyama*, R. Note#, A. Inoue#, and S. Kimura†

Graduate School of Engineering, Nagoya University, Furo-cho, Chikusa, Nagoya 464-8603
**Faculty of Engineering, Himeji Institute of Technology, Shosha, Himeji 671-2201*
#Institute for Materials Research, Tohoku University, Katahira, Aoba, Sendai 980-8577
†Institute for Molecular Science, Myoudaiji, Okazaki 444-8585

A decagonal Al-Ni-Co quasicrystal has two-dimensional quasiperiodic planes stacked along a 10-fold axis (*c*-axis) with a normal crystalline periodicity. In accordance with the structural anisotropy, its electrical resistivity in the quasiperiodic plane is about ten times larger than that along the c-axis, and increases with decreasing temperature, while the resistivity along the axis decreases [1]. The relatively large resistivity and its negative temperature-dependence have been discussed in terms of a pseudo-gap in the vicinity of the Fermi level and spiky structures of the density of states [2]. On the other hand, the electronic structure of the quasicrystal has been experimentally investigated with use of the photoelectron spectroscopy [3, 4], inverse photoelectron spectroscopy [5], soft X-ray spectroscopy [4, 6], and tunneling spectroscopy [7]. They show lowering of the intensity around the Fermi level in their spectra, which may suggest the opening of a pseudo-gap across the Fermi level. Reflectivity spectra of three-dimensional icosahedral quasicrystals have been also studied, which shows neither Drude- nor semiconductor-type frequency dependence of their optical conductivity [8]. Here, we report a preliminary result on infrared reflectivity measurements of a decagonal single quasicrystal $Al_{72}Ni_{12}Co_{16}$ in order to obtain its optical conductivity and clarify its electronic structure.

Infrared reflectivity spectra for the incident photons polarized linearly in perpendicular and parallel with the *c*-axis, *i.e.* in the quasiperiodic and periodic directions, respectively, were measured with a standard setup of a Fourier interferometer at the beamline 6A1 of UVSOR at the temperatures of 300, 80 and 10 K. Specimens of single quasicrystals grown by a Czochralski method [9] were cut into a size of 5 mm in diameter and 1 mm in thickness, and mechanically polished along or perpendicular to the *c*-axis. Measured area was restricted to 2 mm in diameter by a conical aperture in front of the specimen. In order to correct contributions of such as surface roughness and small scratches and to obtain an absolute value of the reflectivity, we measured infrared reflectivity spectra of gold, evaporated on the same surfaces that were used for the reflectivity measurement of the specimen, and compared them with data in the reference [10].

Infrared reflectivity spectra obtained at the temperature of 300 K are shown in Fig. 1 together with those measured at BL-1 of SOR-RING, the Synchrotron Radiation Laboratory of the Institute for Solid State Physics, the University of Tokyo, in a photon energy range between 2 and 30 eV. Since we measured the photon-energy dependence of the relative reflectivity in the visible-vacuum ultraviolet (VUV) region, the visible-VUV data in the figure is plotted so as to coincide with the infrared data extrapolated to the visible region. These infrared reflectivity spectra are similar to those reported for other decagonal Al-Co-Cu-(Si) quasicrystals [11], which reveal a Drude feature in the optical conductivity for the periodic direction and almost frequency-independent optical conductivity for the quasiperiodic direction. This similarity most likely arises from the long-range ordering of these materials, that is their two-dimensional quasiperiodicity, as well as similarity in the constituent elements. The Drude-like behavior is also seen in the present reflectivity spectrum for the polarization parallel to the *c*-axis below $h\nu = 1$ eV. Reflectivity for the polarization along the quasiperiodic direction is almost unity for the low photon energy, which is different from the three-dimensional quasicrystal [8]. At present, we do not find the semiconductor-like behavior or presence of a pseudo-gap in the spectra. However, we recognize the anisotropy in the reflectivity below the photon energy $h\nu$ of 1 eV, which is apparently consistent with that in the electrical resistivity. By assuming the Drude-type frequency dependence in the low photon energy region for both directions, we can estimate the concentration of free carriers in the periodic direction to be larger than that in the quasiperiodic plane by a factor of about ten. The reflectivity spectra in the visible-VUV region do not show much difference in shape; they start to decrease at around $h\nu = 4$ eV, and show humps at $h\nu = 12$ and 18 eV. This suggests that the electronic structure relevant at least to this photon energy region is similar for both directions parallel and perpendicular to the *c*-axis. The 18-eV structure may be related to the plasmon loss peak

observed in the electron energy loss spectra of quasicrystals [11], and the 12-eV feature might be attributed to an interband transition relevant to the constituent transition metal. For further detailed discussion, we have to obtain optical conductivity or dielectric function by a Kramers-Kronig analysis, which is now in progress and will be reported elsewhere.

References

[1] T. Shibuya *et al.*, *J. Phys. Soc. Jpn.* **59** (1990) 1917.
[2] G. Trambly de Laissardiére and T. Fujiwara, *Phys. Rev.* **B50** (1994) 9843.
[3] Z. M. Stadnik *et al.*, *Phys. Rev.* **B51** (1995) 11358.
[4] K. Soda *et al.*, *Proc. of the 7th Int. Conf. on Quasicrystals, to be published.*
[5] K. Soda *et al.*, *J. Electron Spectrosc. Relat. Phenom., to be published.*
[6] E. Belin-Ferré *et al.*, *J. Phys.: Condens. Matter* **8** (1996) 9213.
[7] D. N. Davydov *et al.*, *Phys. Rev. Lett.* **77** (1996) 3173.
[8] C. C. Homes *et al.*, *Phys. Rev. Lett.* **67** (1991) 2694.
[9] Y. Yokoyama *et al.*, *Sci. Rep. RITU* **A42** (1996) 185.
[10] E. D. Palik (ed.), *Handbook of Optical Constants of Solids*, (Academic Inc., Orlando, 1985).
[11] D. N. Basov *et al.*, *Phys. Rev. Lett.* **72** (1994) 1937.
[12] M. Terauchi *et al.*, *Phil. Mag. Lett.* **74** (1996) 107.

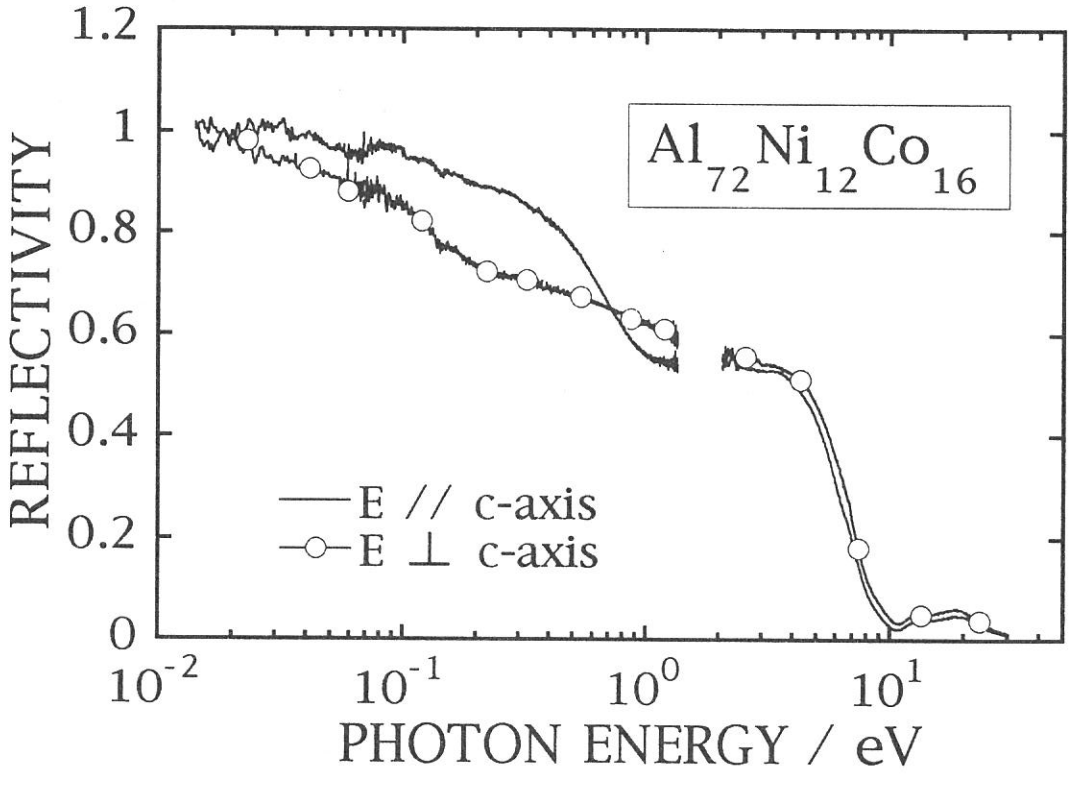

Figure 1. Reflectivity spectra of $Al_{72}Ni_{12}Co_{16}$ for the incident photons polarized in parallel with (solid curve with open circles) and in perpendicular to (solid curve) the c-axis.

(BL6A1)

Infrared magnetic circular dichroism of magnetic exciton of GdAs

Shin-ichi KIMURA, Dexin LI[1], Yoshinori HAGA[2] and Takashi SUZUKI[3]

UVSOR Facility, Institute for Molecular Science, Okazaki 444-8585
[1]Oarai Branch, Institute for Material Research, Tohoku University, Oarai 311-13
[2]Advanced Science Research Center, Japan Atomic Energy Research Institute, Tokai 319-11
[3]Department of Physics, Tohoku University, Sendai 980-77

In the last fiscal year, an infrared magneto-optical apparatus has been constructed at BL6A1 [1]. The main purpose is to measure infrared magnetic circular dichroism (IRMCD) of magnetic materials using circularly polarized infrared synchrotron radiation [2]. The experiment is expected to obtain informations of electronic structures with magnetic moments near the Fermi level. In the case of strongly correlated electron systems, the electronic structure that is made by coupling between carriers and magnetic moments appears near the Fermi level. Then the IRMCD is one of powerful tools for the investigation of such electronic structure.

GdAs is one of strongly correlated electron systems with low-carrier concentration. The physical properties are simple because it is a Heisenberg-type antiferromagnetic material with the Néel temperature of 18.7 K [3]. However, an absorption structure with strong temperature and magnetic field dependences has been found around 0.4 eV [4]. According to the temperature dependence, the absorption is considered to be due to an exciton. However, its magnetic field dependence is anomalous. To investigate the origin of the magnetic field dependence, IRMCD was performed.

Reflectivity spectra with circularly polarized infrared light in the energy range of 10 meV - 2 eV were measured under magnetic field up to 6 T and at the temperature of 6 - 60 K. The measurement was done by using fixed circular polarization direction (left circular polarization) and by using changed magnetic field direction. The reflectivity spectra in the energy range of 2 - 30 eV were measured at BL1B. After the connection of these spectra, optical conductivity spectra were derived from the Kramers-Kronig transformation of the reflectivity spectra. From here and in figures, the spectrum in the case of the magnetic field direction parallel to the polar direction of light is denoted by Δl = +1 and antiparallel is denoted by Δl = -1.

The magnetic field dependences of circularly polarized optical conductivity spectra at 6 K were shown in Fig. 1 (a). Peak energies around 0.4 eV of Δl = ±1 spectra are different from each other, i. e.,

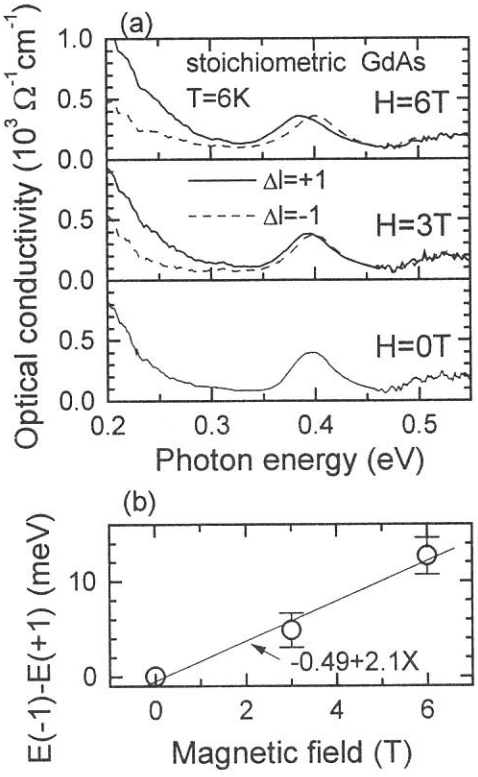

Fig. 1. (a) Magnetic field dependence of circularly polarized optical conductivity spectra at 6 K. Magnetic circular dichroism of absorption at 0.4 eV of GdAs appears. (b) The different energy (E(-1)-E(+1)) between the two peaks of Δl = ±1 as the function of applied magnetic field. The energy difference linearly changes as the magnetic field increases.

magnetic circular dichroism appears in the 0.4 eV absorption of GdAs. The difference between the two peaks ($E(-1)$-$E(+1)$) linearly increases with increasing magnetic field as shown in Fig. 1 (b). This just indicates Zeeman splitting of an exciton. The slope is determined to be 2.1 meV/T by a least square method. The value is about ten times larger than normal electron response. However, since the magnetic field applied to the exciton is induced by Gd^{3+} ions, the induced field should be considered. According to the magnetization data [3], the magnetization has linear response to applied magnetic field up to 13 T. The relation is $M = 0.4\ H$ per Gd^{3+} ion, where M means magnetization and H applied field. From the relation of $E(-1) - E(+1) = 2g\mu_B\ (H + nM)$, where g is g-factor ≈ 2, μ_B Bohr magneton and n the number of Gd^{3+} ion which makes the induced magnetic field to an exciton, the area of one exciton can be determined. The n becomes 20, i. e., one exciton expands in the volume of twenty Gd^{3+} ions.

On the other hand, the temperature dependences of circularly polarized optical conductivity spectra at ±6 T are shown in Fig. 2 (a). In comparison with the spectra at 60 K, the peak energy difference at 6 K is larger. The energy difference is plotted in Fig. 2 (b). The splitting energy increases as the temperature decreases above 20 K. However, the energy difference becomes almost constant below 20 K. Since the Néel temperature of GdAs is 18.7 K, the change of the slope comes from the magnetic transition. Therefore, the Zeeman splitting of the exciton is a signal of the magnetic transition.

---

[1] S. Kimura, UVSOR Activity Report 1996 (1997) p. 170.

[2] S. Kimura, in this issue.

[3] D. X. Li, Y. Haga, H. Shida, T. Suzuki, T. Koide and G. Kido, Phys. Rev. B **53** (1996) 8453.

[4] S. Kimura, D. X. Li, Y. Haga and T. Suzuki, UVSOR Activity Report 1996 (1997) p. 172; J. Magn. Magn. Mater. **177-181** (1998) in press.

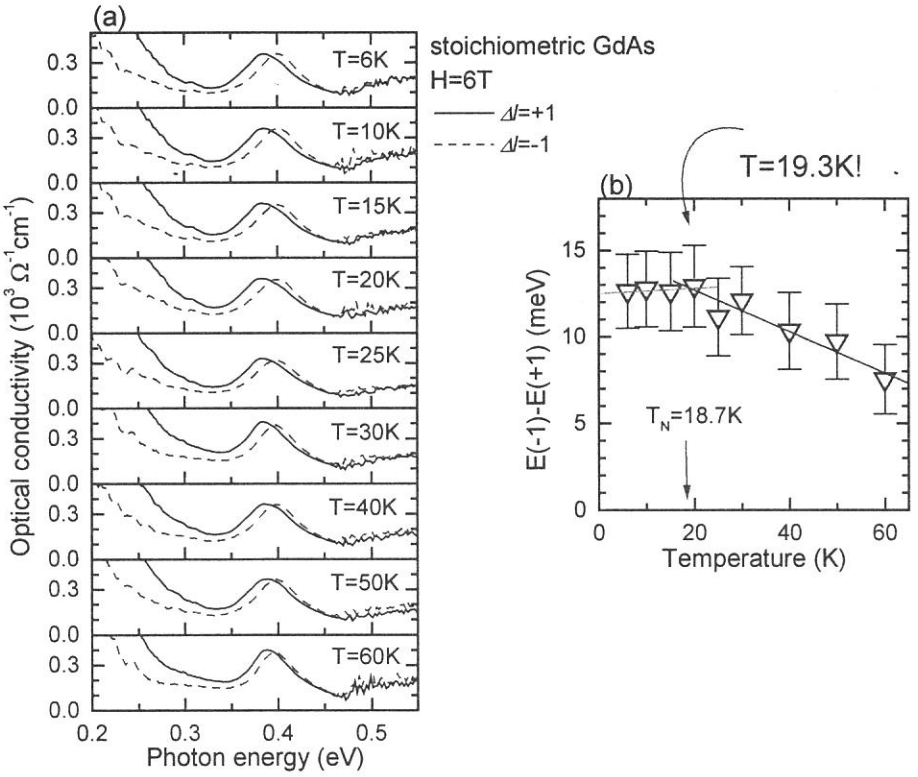

Fig. 2. (a) Temperature dependence of circularly polarized optical conductivity at ±6 T. (b) The energy difference of two peaks of $\Delta l = \pm 1$ as the function of temperature.

(BL6A1)

Heavy-Fermion-Like Optical Conductivity of Yb_4As_3

Shin-ichi KIMURA, Akira OCHIAI[1], and Takashi SUZUKI[2]

UVSOR Facility, Institute for Molecular Science, Okazaki 444-8585
[1]Department of Material Science and Technology, Niigata University, Niigata 950-21
[2]Department of Physics, Tohoku University, Sendai 980-77

Yb_4As_3 is a typical strongly correlated 4*f*-electron system with low carrier concentration. The temperature dependence of optical conductivity (OC) spectrum has been measured in the photon energy of 2 meV – 50 eV at several temperature of 39 – 320 K in the last fiscal year [1]. The result indicates that there is an absorption with strong temperature dependence around 0.4 eV. The electronic structure from which the absorption originates crosses the Fermi level and changes to conduction band with short relaxation time. Physical properties at higher temperature come from the electronic structure. After that, we measured reflectivity spectra at several temperatures down to 6 K form the investigation of the electronic structure at lower temperature and reported here.

Reflectivity spectra were measured at an infrared beam line 6A1. The magneto-optical system which was constructed in the last fiscal year [2] was used in spite of no magnetic field because measuring of temperature dependence below 100 K is easier than normal optical system of BL6A1. We discuss using OC spectra that were determined from a Kramers-Kronig analysis of the reflectivity spectra.

The OC spectra at several temperatures are shown in Fig. 1. The spectra are plotted with the DC conductivity and the carrier number derived from the Hall coefficient. Above 700 meV, the OC spectra originates from interband transitions. Therefore the temperature dependence is small. On the other hand, below 700meV, the spectrum strongly changes with temperature. The origin of a peak at 0.4 eV has already discussed [1] and mentioned before. Here, we discuss the origin of structures below 8 meV and around 30 meV. Note that some sharp peaks around 15 meV come from TO phonons. We do not discuss them in this

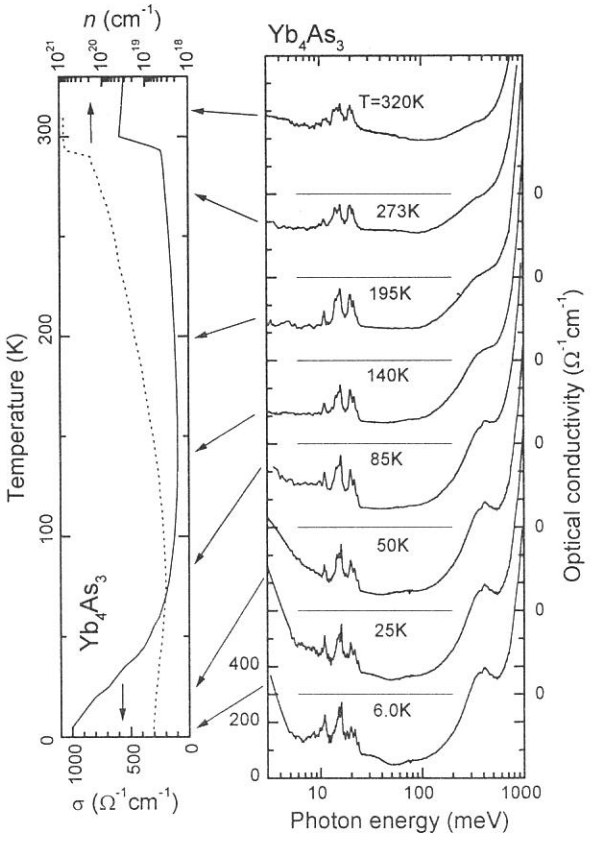

Fig. 1. Temperature dependence of optical conductivity spectrum of Yb_4As_3 with the DC conductivity and the carrier number derived from the Hall coefficient.

report.

Drude-type optical conductivity appears below 8 meV. From the carrier number and the DC conductivity, we can get a Drude function,

$$\sigma(\omega) = \left(\frac{Nm_0}{m^*}\right)\frac{e^2\tau}{m_0(\omega^2\tau^2+1)}$$

with a parameter of the effective mass, m^*. After the fitting, the effective mass is determined to be $0.7m_0$, which is equal to that of cyclotron mass derived from microwave resonance [3]. The relaxation time is 3.1×10^{-12} sec, which value is hundred times larger than that of normal metals.

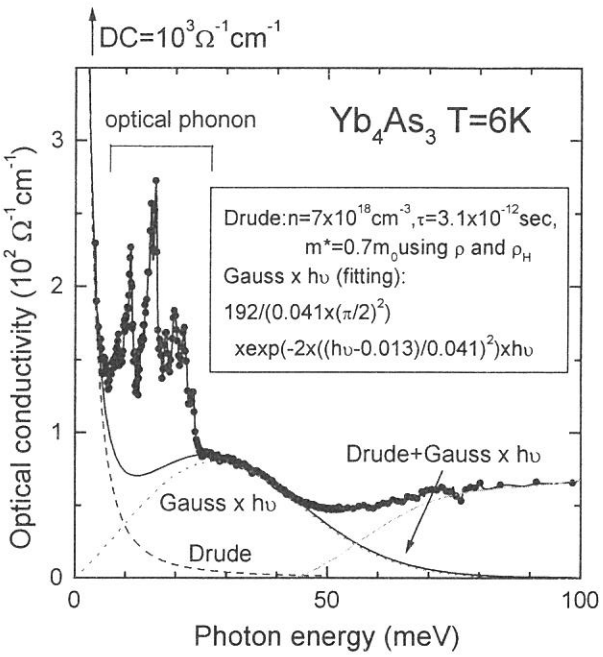

Fig. 2. Optical conductivity spectrum of Yb_4As_3 at 6 K and the fitting curves.

Around 30 meV, a shoulder develops as temperature decreases. Then we fitted the spectrum of 25 - 45 meV at 6 K. We can get a good fitting by a function of Gaussian×$h\nu$. The fitting function shows there is a peak around 30 meV, i. e., a small gap opens on the Fermi level.

According to a theory of Coleman [4], the spectrum can be explained by a Kondo lattice model. The Kondo temperature (T_K) of Yb_4As_3 is estimated to be about 100 K (8.6 meV) by the DC conductivity. Therefore the width of Drude part becomes 1 T_K and the energy of the gap becomes 3 T_K. The results are equal to the theory of Coleman. However, it is thought that the charge of Yb_4As_3 does not couple with the magnetism [5]. And also similar spectrum shape appears in organic materials, which originates from the CDW nature. Therefore the origin of the spectrum shape should be considered.

---

[1] S. Kimura, M. Ikezawa, A. Ochiai and T. Suzuki, J. Phys. Soc. Jpn. **65** (1996) 3591; S. Kimura, A. Ochiai and T. Suzuki, UVSOR Activity Report 1996 (1997), p. 174.
[2] S. Kimura, UVSOR Activity Report 1996 (1997), p. 170.
[3] H. Matsui *et al.*, private communication.
[4] P. Coleman, Phys. Rev. Lett. **59** (1987) 1026.
[5] A. Ochiai, private communication.

(BL6A1)

Optical reflectivity study of the Kondo insulator YbB_{12}

H. Okamura, H. Sinozaki, T. Nanba, S. Kimura[A],
F. Iga[B], N. Simizu[B] and T. Takabatake[B]

Department of Physics, Kobe University, Kobe 657-8501.
[A]UVSOR, Institute for Molecular Science, Okazaki 444
[B]Department of Materials Science, Hiroshima University, Higashi-Hiroshima 739

YbB_{12} is one of the strongly correlated electron systems known as "Kondo insulators".[1] It is paramagnetic at high temperatures, but with lowering the temperature below 75 K, χ decreases and the electrical resistivity (ρ) increases. The temperature dependences of both χ and ρ show thermally activated behaviors, and indicate the presence of an energy gap of about 10 meV. These unique behaviors are believed to arise from strong interactions between the localized f-electrons and free carriers, but the mechanism responsible for them is not exactly known yet. In particular, it is important to obtain more information about the behaviors of energy gap at low temperatures. Although infrared reflectivity measurements are very useful for this purpose, earlier optical measurements on YbB_{12} suffered from a lack of high-quality single crystal.[2,3] Recently, however, Iga, Shimizu and Takabatake have successfully grown single crystals of YbB_{12} [4]. Using BL6A1 we have measured the optical reflectivity of single crystals of YbB_{12} at various temperatures between 20 K and 300 K. Figure 1(a) shows the reflectivity spectrum of YbB_{12} at 290 K, 160 K, 78 K, and 20 K, and Fig. 1(b) shows the corresponding optical conductivity $\sigma(\omega)$ obtained from the reflectivity spectra via Kramers-Kronig analyses. At 290 K, there is a strong absorption peaked around 0.2 eV, superimposed on a broad, Drude-like free carrier contribution. This absorption peak at 0.2 eV is not seen for LuB_{12}, which has a filled f-shell and non-magnetic, and is likely to arise from f-levels located near the Fermi level. Upon cooling, the free carrier contribution is rapidly suppressed, and below 80 K the spectral weight below 20 meV in $\sigma(\omega)$ is completely depleted. Figure 2 shows the detailed temperature dependence of the gap structure seen in $\sigma(\omega)$ below 80 K. From this we can see that the gap structure in $\sigma(\omega)$ appears just below 78 K. This temperature nearly coincides with the temperature below which χ decreases rapidly, hence the gap appearance seen in $\sigma(\omega)$ is correlated with the magnetic properties. To clarify further the characteristics of the energy gap, we plan to study the reflectivity of $Yb_{1-x}Lu_xB_{12}$ with several values of x, including their response to magnetic field.

References

[1] G. Aeppli and Z. Fisk, Comments Cond. Mat. Phys. **16**, 155 (1992).

[2] P. Wachter and G. Travaglini, J. Magn. Magn. Mater. **47&48**, 423 (1985).

[3] H. Okamura et al, UVSOR Annual Report 1997, p162.

[4] F. Iga, N. Shimizu, and T. Takabatake, J. Magn. Magn. Mater. to be published.

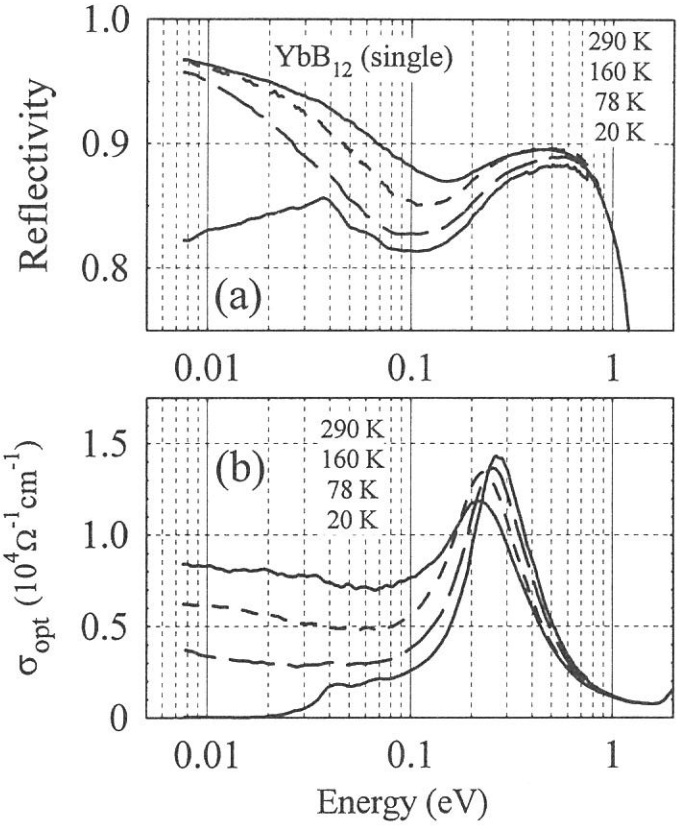

Fig.1: Reflectivity (a) and optical conductivity (b) of YbB_{12} single crystal at several temperatures.

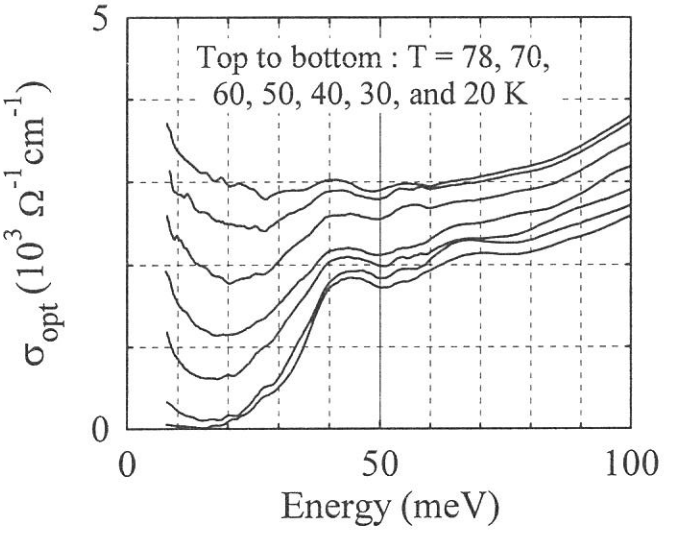

Fig. 2: Optical conductivity of YbB_{12} below 78 K.

(BL6A1)

Millimeter Wave Reflection Measurement of Secondary Battery Substance $LiNiO_2$

Hitoshi OHTA, Yoji IKEUCHI, Shunsuke ONO, Takao NANBA, Atushi HIRANO* and Ryoji KANNO*

Department of Physics, Faculty of Science, Kobe University,1-1 Rokkodai, Nada, Kobe 657

**Department of Chemistry, Faculty of Science, Kobe University,1-1 Rokkodai, Nada, Kobe 657*

Nowadays Li ion secondary battery has attracted much attention because it is a promising secondary battery due to its high energy density and light weight.[1] Although $LiCoO_2$ is already in commercial use as an electrode material in secondary Li batteries, $LiNiO_2$ is a promising candidate to replace $LiCoO_2$ from the economical point of view. This is due to the fact that Ni atoms is cheaper and easy to obtain than Co atoms. However, the composition of $LiNiO_2$ is very sensitive to the synthesis condition, especially the sintered temperature, and it can be easily lead to a decomposition to $Li_{1-x}Ni_{1+x}O_2$. The non-stoichiometry degrades the charge and discharge characteristics significantly. However, Kanno *et al.* succeeded in synthesizing nearly stoichiometric $LiNiO_2$ and they opened the way to use $LiNiO_2$ as an electrode material in secondary Li batteries.[2] The aim of our study is to obtain the information about the diffusive motion of Li^+ ions by observing "ionic plasmon" whose existence can be proved as a definite increase in a reflectivity towards a low energy side in the millimeter wave region because the mass of Li^+ ion is larger than that of electron. The first observation of ionic plasmon has been performed previously for alkali silver iodide super-ionic conductors MAg_4I_5 (M=Rb, K and NH_4) by Awano *et al.*[3]

The reflection measurements of the nearly stoichiometric $LiNiO_2$ sintered at 650°C has been performed in the spectral region from 6 to 50 cm^{-1} using the beam line BL6A1 of UVSOR. Low pass filter below 22 cm^{-1} was used for the low energy region. The temperature was varied from 79 K to 380 K and the liquid He cooled InSb detector was used. Figure 1 shows the results of our measurements. The reflection is almost flat for the observed region below 197 K. The previous measurements also showed similar behavior for 11 K.[4] However, the reflection in the low energy region increases monotonically as the temperature is increased above 300 K. This result is consistent with the fact that diffusive motion of Li^+ ions is low at low temperature but starts to increase above 300 K. Therefore the temperature dependence strongly suggests that the increase of the reflection in the low energy side is due to the ionic plasmon of Li^+ ion. The detailed analysis of the data is underway.

Acknowledgments: One of the authors (HO) is grateful to Murata Science Foundation for the financial support.

References

[1] S. Megahed and B. Scrosati: The Electrochemical Society Interface, Winter (1995) 34.

[2] R. Kanno *et al.*: J. Solid State Chem. **110** (1994) 216.

[3] T. Awano *et al.*: Solid State Ionics **53-56** (1992) 1269.

[4] H. Ohta et al.: UVSOR Activity Report (1996) 182.

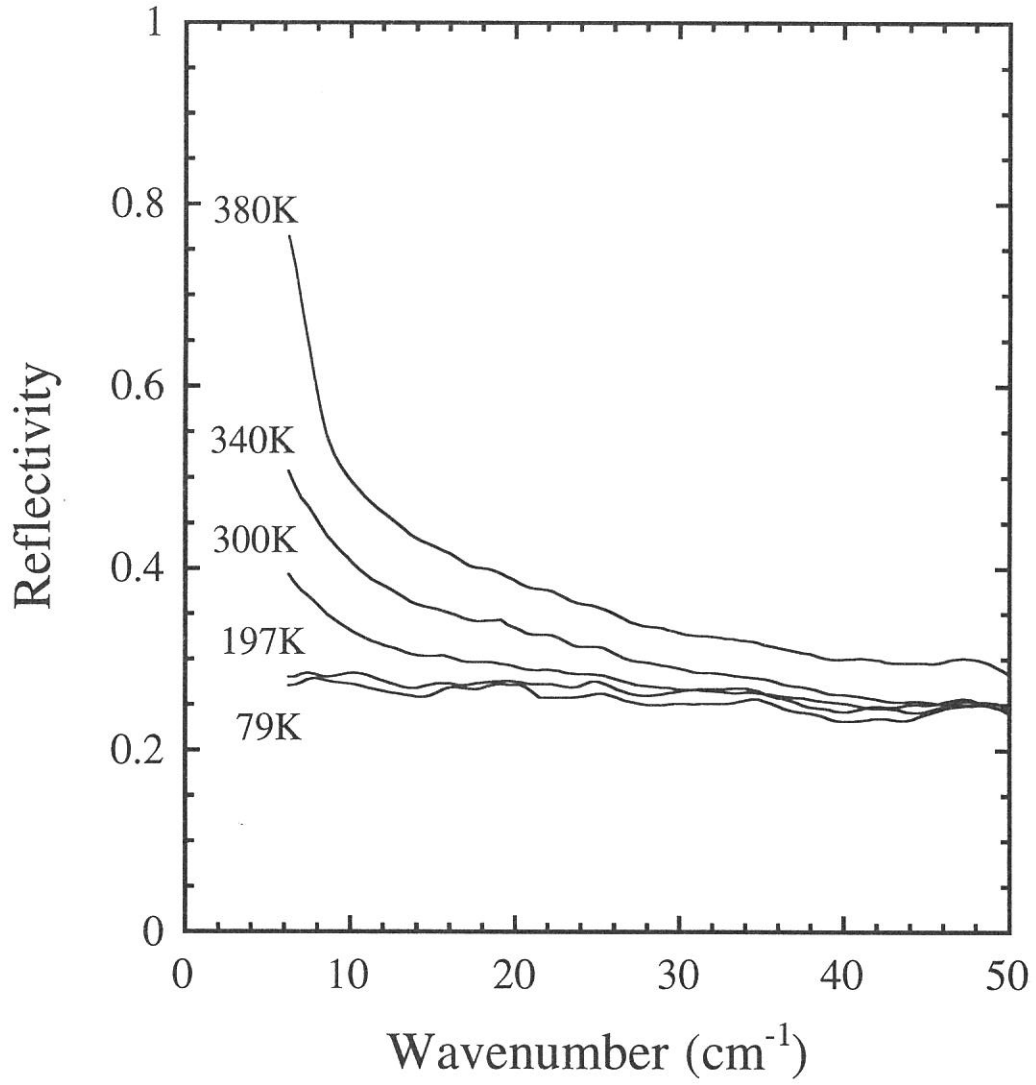

Fig. 1 The reflection spectra of the nearly stoichiometric $LiNiO_2$ sintered at 650°C.

(BL6A1)

Far-infrared Reflection Spectrum of Ice Ⅷ

Masato Hayashi and Takao Nanba[A]

Faculty of Natural Science , Kobe University, Nada-ku, Kobe 657-8501
[F]*aculty of Science, Kobe University, Nada-ku, Kobe 657-8501*

Ice has more than ten stable phase according to the environment of pressure and temperature. At Ⅶ, the oxygen atom of the hydrogen molecule forms two net works with a diamond structure (Fig.1). Two net works intersect each other and the position of the proton atoms is in disorder. At Ⅷ, on the other hand, the oxygen atoms form the same two net works with a diamond structure, but the position of proton forming the hydrogen bonding with oxygen atom is in order. Consequently, Th. orientation of the dipole moment of the water molecule in the one net work has the same direction and the one in the other net work has the opposite direction. That is, the only difference between two phases in structure is the order-disorder on the proton configuration.

Hitherto, various types of spectroscopic studies have been done on ice. However, the far infrared spectroscopy on ice under pressure has not been done except only one [1] because of the difficulty in doing the experiment using a diamond anvil cell (DAC). The transmission light intensity through DAC is too weak to detect. Kobayashi *et al* made the transmission measurement on very thin ice at low temperature and observed the anomalous pressure dependence of the phonon frequencies of ice at the phase Ⅷ[1]. Unfortunately, the signal showed a saturation around the region of the absorption peak due to the infrared active phonon mode because of the strong absorption. We made a far-infrared reflection measurement on ice under pressure using a DAC and synchrotron radiation (UVSOR) , and succeeded ,for the first time, to measure the change in the far-infrared reflection spectra on ice due to the phase transition between Ⅶ and Ⅷ phases.

Fig.2 shows the developments of the power spectra on ice under pressure in the far-infrared region. The sample was compressed up to 2.6 GPa at room temperature (Ⅶ) and then cooled down to Ⅷ phase. A new peak was resolved around 220 cm^{-1} at Ⅷ phase which corresponds to the TO phonon mode at Ⅷ phase. The ratios of spectra at Ⅷ phase to that at Ⅶ phase was shown in Fig.3. The peak at Ⅷ phase showed a blue shift of about 17 cm^{-1}/GPa to pressure .

[1] M.Kobayashi; Solid State Physiscs (Japan) 31,(1996)127.

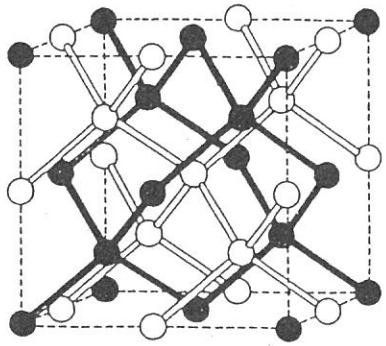

Fig.1 Crystal structure of ice at Ⅶ and Ⅷ phases. The open and closed circles corespond to oxgen atoms and show two net works with a diamond structure.

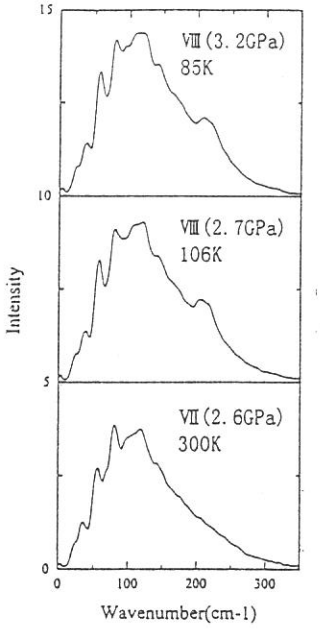

Fig.2 shows the development of the spectra of ice under pressure.

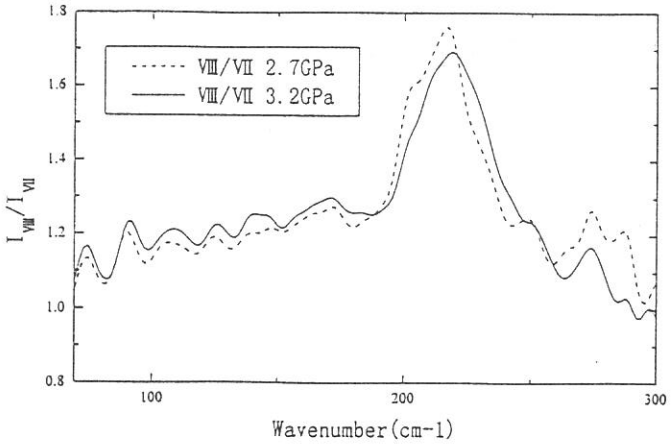

Fig.3 shows the ratios of spectra at Ⅷ phase at 2.7(dot) and 3.2 GPa(solid curve) to that at Ⅶ phase.

(BL6A1)

IR reflection and magneto-reflection of the $Yb_4(As_{1-x}Sb_x)_3$ system

Raniero Pittini [a], Mikihiko Ikezawa [a], Akira Ochiai [b], Hidekazu Aoki [c] and Takashi Suzuki [c]

[a] *Research Institute for Scientific Measurements, Tohoku University, Sendai 980-77, Japan*
[b] *Department of Material Science and Technology, Niigata University, Niigata950-21, Japan*
[c] *Department of Physics, Faculty of Science, Tohoku University, Sendai 980-77, Japan*

After the study of the optical response of $Yb_4(As_{0.88}Sb_{0.12})_3$ and $Yb_4(As_{0.71}Sb_{0.29})_3$ performed extensively last year over a wide energy range from 1 meV to 5.5 eV, this year we focused on two points, i.e. *a*) the temperature dependence of the IR optical signal (in the photon energy region of the free carrier absorptions and phonon absorptions) and *b*) the field dependence of the optical absorption of the $4f \rightarrow 5d$ transitions.

a) Temperature dependence of the IR optical signal

The free carrier contributions to the optical signal can be fitted with a Drude model, yielding the plasma frequency ω_p and the scattering rate γ as parameters. Repeating this fit for all the measured temperatures, one can determine the effective mass of the charge carriers from the plasma frequency, taking the carrier density from the Hall data. The result is shown in Fig. 1.

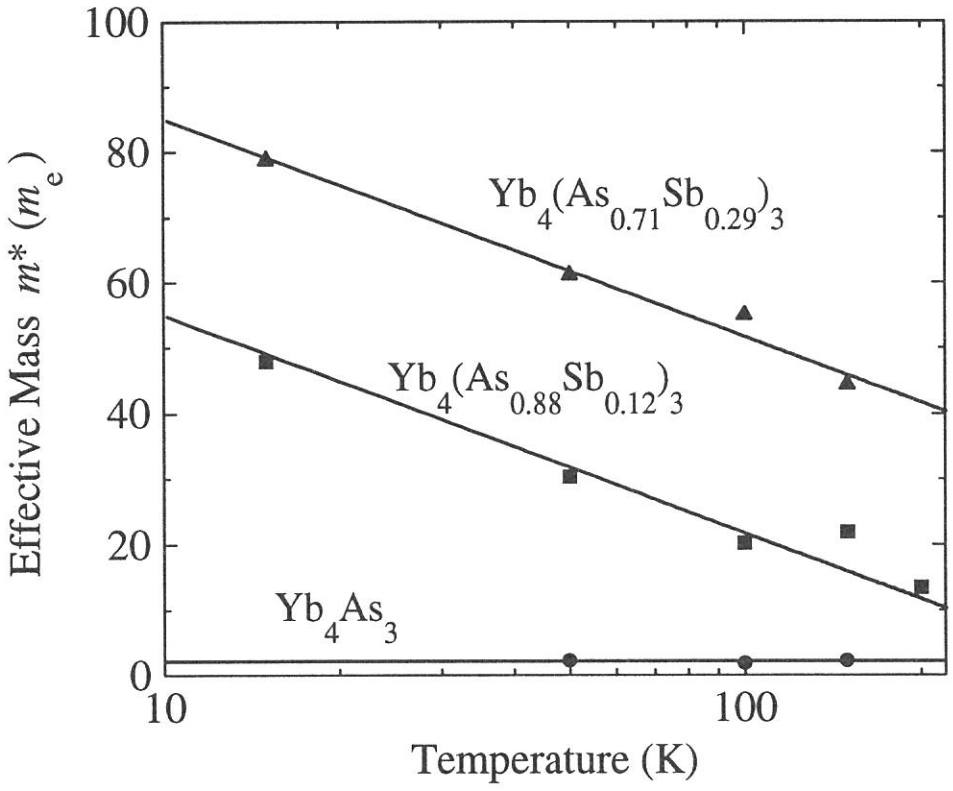

Fig. 1: Temperature dependence of the effective mass in the Yb_4X_3 system, obtained from the optical data (R. Pittini et al., ICM'97, scheduled for J. Magn. Magn. Mat. **177-181** (1998)).

The effective mass of the carriers in Yb_4As_3 is not particularly enhanced and temperature independent, while the effective masses in $Yb_4(As_{0.88}Sb_{0.12})_3$ and $Yb_4(As_{0.71}Sb_{0.29})_3$ have a logarithmic temperature dependence, and reach the values of 55 m_e and 85 m_e at 10 K, respectively. Therefore, the Sb-substituted samples are nearer to a heavy fermion than 'pure' Yb_4As_3.

b) Field dependence of the optical absorption of the $4f \rightarrow 5d$ transitions

The magneto-reflection of the $4f \rightarrow 5d$ transitions in $Yb_4(As_{0.88}Sb_{0.12})_3$ and $Yb_4(As_{0.71}Sb_{0.29})_3$ is very strong (Fig. 2), in particular the sharp peak at 0.4 eV. This indicates that the magnetic dichroism is strong in the Sb-substituted samples, while it appears to be weak in 'pure' Yb_4As_3. For the peaks between 0.1 and 0.3 eV and at 0.5 eV, the origin is still unclear. But similar effects have been reported recently at very high fields in low dimensional systems (J.S. Brooks, RHMF'97). The Yb_4X_3 materials are indeed low dimensional systems, as the $4f$ bands are one-dimensional. But the $Yb_4(As_{1-x}Sb_x)_3$ system is particular because the anomalies appear already at moderately low fields.

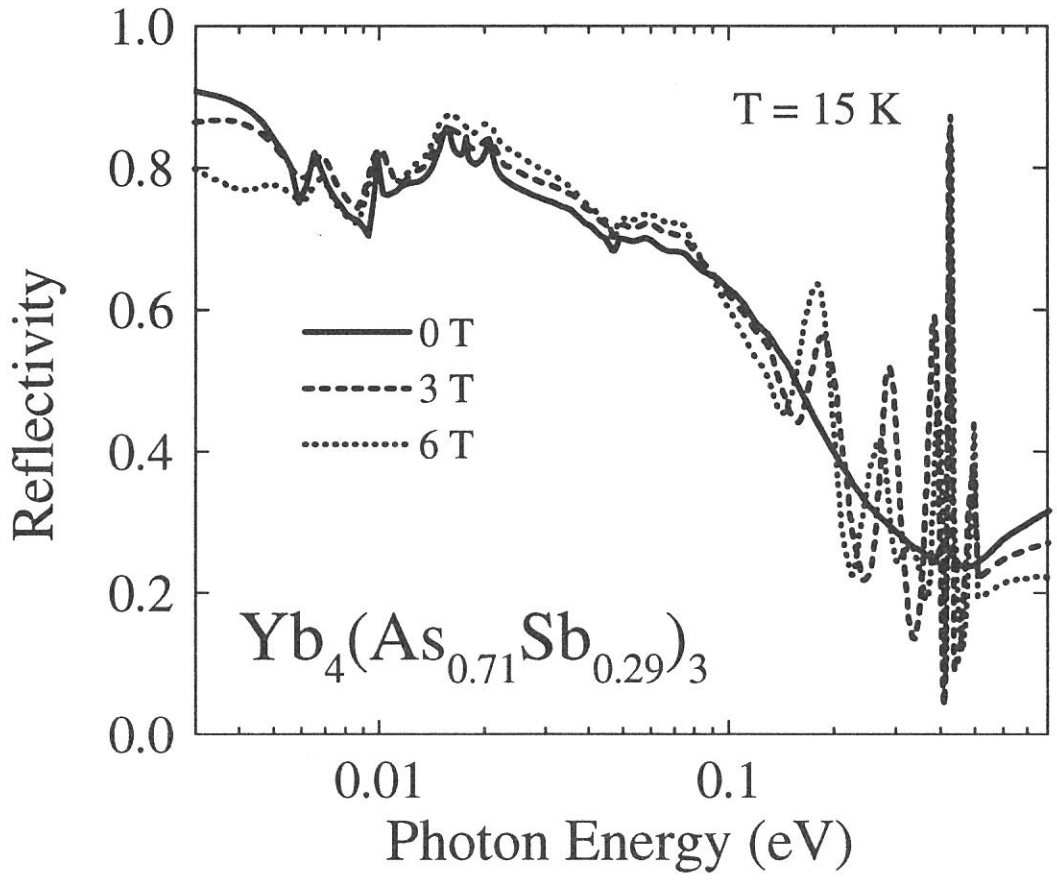

Fig. 2: Field dependence of the optical reflection in $Yb_4(As_{0.71}Sb_{0.29})_3$ at 15 K. (R. Pittini et al., RHMF'97, to be published in Phys. B).

(BL6A1)

Millimeter Wave Spectroscopy of Superionic Conducting Glasses

Naotake Sasaki, Katsuyoshi Handa and Teruyoshi Awano

Department of Applied Physics, Tohoku Gakuin University, Tagajo 985-0873

There are few precise optical measurements of superionic conducting glasses in the spectral region between millimeter wave and far-infrared. An optical absorption band by a collective motion of mobile ions may appear in this spectral region, in which motion of mobile ions switches from translation to vibration. Such collective motion may be one reason of the high ionic conductivity of these glasses even at low temperature.

We had investigated far-infrared and millimeter wave spectra of some silver or copper ion conductors to study the dynamics of mobile ions. In AM_4X_5 (A=alkali metal; M=Ag or Cu; X=halogen) crystal, a structure by "ionic plasmon" was observed in the spectral region below 10 cm^{-1} in silver ion conductors or 30 cm^{-1} in copper ion conductors in energy loss function spectra at temperatures of superionic conducting phase[1].

In this study, we report results on $(AgI)_x(AgPO_3)_{1-x}$, $(TMAI)_{0.1}(TEAI)_{0.1}(AgI)_{0.8}$, (TMAI=$(CH_3)_4NI$, TEAI=$(C_2H_5)_4NI$) superionic conducting glasses comparing the results of copper ion conducting glasses in the millimeter wave region. Large alkylammonium ions disperse randomly into AgI in organic-inorganic glasses in contrast to oxide tetrahedrons in inorganic glasses.

Optical constants were obtained from reflectivity spectra by K-K analysis. In the millimeter wave region, the transmittance spectra of samples with different thickness were measured directly. Absorption coefficient spectra of this spectral region were calculated from them.

Fig. 1 shows AgI composition dependence of intensity of absorption bands in millimeter wave region. As the AgI composition decreased, the absorption intensity around 7 cm^{-1} decreased. Fig. 2 shows temperature dependence of this absorption band. The 7 cm^{-1} band decreased as temperature decreased. This suggest that the absorption around 7 cm^{-1} is due to a sort of diffusive motion of conduction ions. The 7 cm^{-1} band in AgI-$AgPO_3$ shifted to 9 cm^{-1} in CuI-$CuPO_3$. The square root of mass ratio of silver and copper ion is 1.3. Therefore the wave number shift of these absorption bands means that these bands are due to movements of conduction ions.

Fig. 3 shows the spectral change of the absorption spectra in millimeter wave region of $(TMAI)_{0.1}(TEAI)_{0.1}(AgI)_{0.8}$ glass as temperature decreased. The same spectral change as AgI-$AgPO_3$ was observed. Fig. 4 shows spectral change of the absorption band in millimeter wave region between $(TMAI)_{0.1}(TEAI)_{0.1}(AgI)_{0.8}$ and $(TMAI)_{0.15}(TEAI)_{0.1}(CuI)_{0.75}$. The 8 cm^{-1} peak in $(TMAI)_{0.1}(TEAI)_{0.1}(AgI)_{0.8}$ shifted to 11 cm^{-1} in $(TMAI)_{0.15}(TEAI)_{0.1}(CuI)_{0.75}$. This shift coincides with the inverse square root of mass ratio of sliver and copper. This suggest that this band is due to a motion of conduction ions.

The absorption band in millimeter wave region is due to a sort of diffusive motion of conduction ions. Detail of this motion of conduction ions is under investigation.

References

1) T. Awano, T. Nanba and M. Ikezawa, Solid State Ionics, **53-56**, 1269 (1992).

2) J. Kawamura et al., Solid State Ionics, **86-88**, 517 (1996).

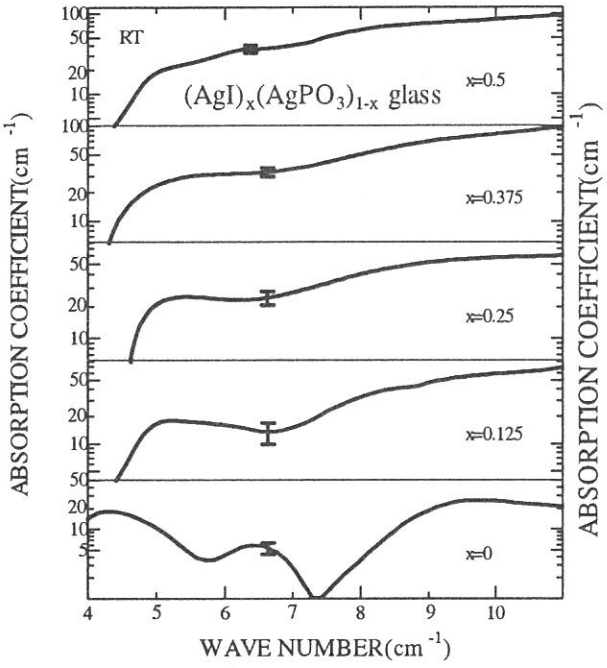

Fig. 1. Spectral change in millimeter wave region of $(AgI)_x(AgPO_3)_{1-x}$ to AgI composition.

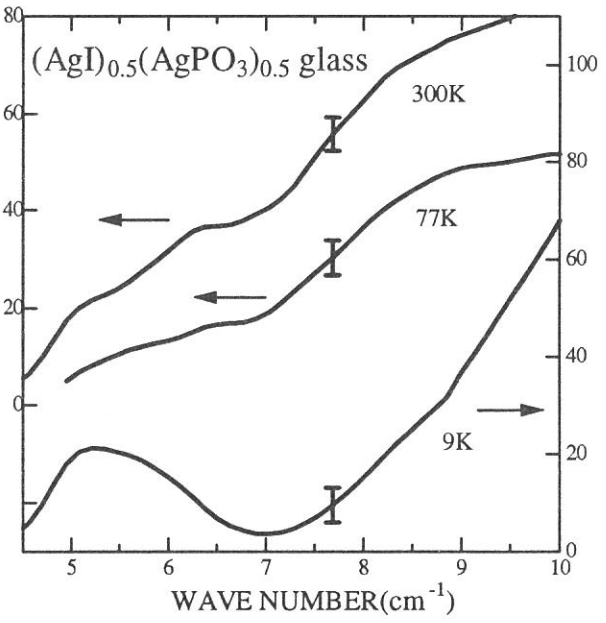

Fig. 2. Spectral change in millimeter wave region of $(AgI)_x(AgPO_3)_{1-x}$ to temperature.

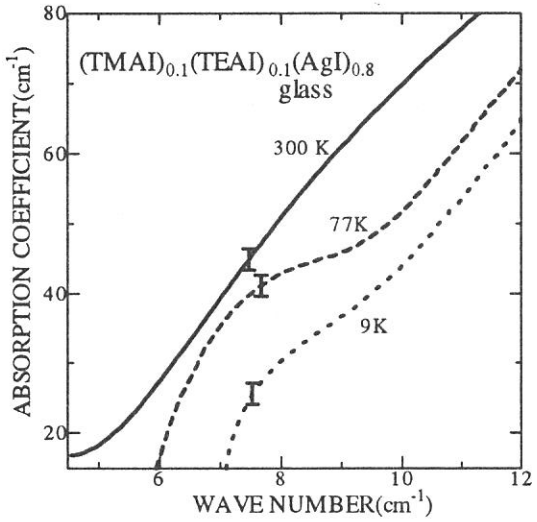

Fig. 3. Spectral change in millimeter wave region of $(TMAI)_{0.1}(TEAI)_{0.1}(AgI)_{0.8}$ to temperature.

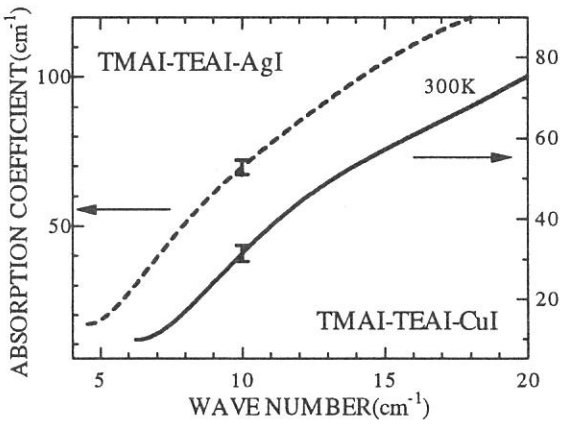

Fig. 4. Spectral change between $(TMAI)_{0.1}(TEAI)_{0.1}(AgI)_{0.8}$ and $(TMAI)_{0.15}(TEAI)_{0.1}(CuI)_{0.75}$ in millimeter wave region.

(BL6A1)

Effect of Photo-excited Carriers on Infrared Reflectivity in InGaN Single Quantum Well Structures

Takahiro DEGUCHI, Takayuki SOTA, Shigefusa CHICHIBU[A],
Takashi AZUHATA[B], Shingo ONO[B], Shinji IZUMIDA[B], Hideyuki OHTAKE[B],
Nobuhiko SARUKURA[B], and Shuji NAKAMURA[C]

Department of Electrical, Electronics, and Computer Engineering, Waseda University, 3-4-1 Ohkubo, Shinjuku, Tokyo 169-8555, Japan
[A]Faculty of Science and Technology, Science University of Tokyo, 2641 Yamazaki, Noda, Chiba 278-8510, Japan
[B]Laser Research Center, Institute for Molecular Science, 38 Nishigonaka, Myodaiji, Okazaki, Aichi 444-8585, Japan
[C]Department of Research and Development, Nichia Chemical Industries Ltd., 491 Oka, Kaminaka, Anan, Tokushima 774-8601, Japan

Recent development of growth techniques for GaN and related nitrides has realized the commercial production of superbright blue and green light emitting diodes based on InGaN single quantum wells, [1] and the room temperature cw operation of InGaN multi-quantum-well laser diodes in the purplish-blue energy region. [2] The life time of laser diodes is more than 10,000 hours. [3] Although it has been reported the excitons localized into certain potential minima caused by the fluctuation of In mole fraction in InGaN contribute to the spontaneous emission in the purplish-blue, blue, and green light emitting diodes, [4,5] the lasing mechanism in the purplish-blue laser diodes is not clear at present. It is important to study the effect of carriers created in InGaN quantum wells.

We investigated the reflectivity change of InGaN single quantum well structures in the infrared region, which would be caused by photo-excited carriers. The samples used here were prepared by the two-flow metalorganic chemical vapor deposition method [6] on the c-plane of sapphire substrates with low-temperature-grown GaN buffer layers. The exact sample structure was p-GaN(0.5 μm)/p-AlGaN(100 nm)/$In_xGa_{1-x}N$(3 nm)/n-GaN(4 μm)/GaN buffer(30 nm)/sapphire substrate. The values of x were 0.3 and 0.45, which correspond to blue and green light emitting diodes, respectively. Infrared reflectivity spectra were measured using BL6A1 at room temperature and 80 K. As light sources to create carriers, 325.0 nm line of a He-Cd laser and 476.5, 488.0, and 514.5 nm lines of an Ar^+ laser were used. Maximum powers for respective lines were 0.02, 1.2, 3.1, and 1.2 W.

The infrared reflectivity spectra measured without laser irradiation show intrinsic phonon structures from GaN layers. The signal from InGaN layer was too thin to be observed. When the laser was irradiated, unfortunately, no change were observed. Some of possible reasons are that the laser powers were too low to cause observable reflectivity changes and that the absorption coefficient of the samples in the visible wavelength region was too small to excite carriers effectively.

The authors are grateful to Dr. S. Kimura for his experimental support, and also to Profs. H. Nakanishi and K. Suzuki and Monsieur T. Gejo for their continuous encouragement.

[1] S. Nakamura, M. Senoh, N. Iwasa, S. Nagahama, T. Yamada, and T. Mukai, Jpn. J. Appl. Phys. 2 **34**, L1332(1995).
[2] S. Nakamura, M. Senoh, S. Nagahama, N. Iwasa, T. Yamada, T. Matsushita, Y. Sugimoto, and H. Kiyoku, Appl. Phys. Lett. **69**, 4056(1996); S. Nakamura, M. Senoh, S. Nagahama, N. Iwasa, T. Yamada, T. Matsushita, Y. Sugimoto, and H. Kiyoku, Jpn. J. Appl. Phys. 2 **36**, L1059(1997).
[3] S. Nakamura, M. Senoh, S. Nagahama, N. Iwasa, T. Yamada, T. Matsushita, H. Kiyoku, Y. Sugimoto, T. Kozaki, H. Umemoto, M. Sano, and K. Chocho, the 2nd International Conference on Nitride Semiconductors, Tokushima, Japan, 1997.
[4] S. Chichibu, T. Azuhata, T. Sota, and S. Nakamura, Appl. Phys. Lett. **69**, 4188(1996).
[5] Y. Narukawa, Y. Kawakami, Sz. Fujita, Sg. Fujita, and S. Nakamura, Phys. Rev. B **55**, R1938(1997).
[6] S. Nakamura, Y. Harada, and M. Senoh, Appl. Phys. Lett. **58**, 2021(1991).

(BL6A1)

Complex refractive index measurement of various semiconductors in the far-infrared region

Hideyuki OHTAKE, Takashi AZUHATA, Shingo ONO[A], Takeyo TSUKAMOTO[A],
Zhenlin LIU, Shinji IZUMIDA, Takahiro DEGUCHI[B], Takayuki SOTA[B],
and Nobuhiko SARUKURA

Laser Research Center for Molecular Science,
Institute for Molecular Science (IMS), Myodaiji, Okazaki 444-8585,
[A]Faculity of Science, Department of Applied Physics, Science University of Tokyo,
1-3, Kagurazaka, Shinjuku, Tokyo 162-0825
[B]Department of Electrical, Electronics and Computer Engineering, Waseda University,
3-4-1, Ohkubo, Shinjuku, Tokyo 169-8555

The devices and applications to ultrafast opt-electronics of THz radiation or far infrared light from various devices have been intensively studied. [1,2] For the design of various devices in the THz-radiation region, precise information of material properties is strongly required. In particular, precise index refractive and optically and electrically induced index change of typical semiconductors are matter of interest. However, there were few reliable reports of such complex index measurement in the THz-radiation region. Development of complex index measurement system in the far infrared region will open up possibilities for the material research of new high-speed opt-electric devices utilizing THz radiation. There are a few reports[4] that describe how photoexcited carriers in semiconductors change complex-index in the far-infrared region. These works [4,5] have led to not only picosecond time resolved index change measurement [6] but also THz-tomography [7] and THz-ranging[8].

We measured reflectivity change of GaAs and InAs in the THz-region at room and liquid nitrogen temperature by irradiating an Ar ion laser (e.g. 488 nm to 514.5 nm) and HeCd laser light. Infrared reflectivity spectra were obtained by using BL6A1. We investigated exciting wavelength dependence of infrared reflectivity. At room temperature, we did not observe any changes among them. It means that the number of photoexcited carriers in GaAs and InAs do not have any excitation wavelength dependence, because their carrier densities are almost the same due to penetration depths. At liquid nitrogen temperature, unfortunately, we can not obtain reasonable data. Some possible reasons are that the laser power was so high that local heating effect took place and that As component vaporized by heat. To overcome these problems, we should make thin semiconductor films or well defined clear semiconductor surfaces preparing in ultra high vacuum.

The authors are grateful to Dr. S. Kimura for his helpful experimental support, and also to Dr. T. Gejo for his strong encouragement.

References

[1] D. H. Auston, Appl. Phys. Lett. 43, 713 (1983).
[2] P. C. M. Planken, M. C. Nuss, W. H. Knox, D. A. B. Miller, and K. W. Goossen, Appl. Phys. Lett. 61, 2009 (1992).
[3] P. B. Corkum and D. Keith, J. Opt. Soc. Am. B2, 1873 (1985).
[4] H. Ohtake, Z. Liu, S. Izumida, T. Yamanaka, N. Sarukura, K. Koyama, and T. Suemoto, CLEO Pacific Rim '97, paper P50.
[5] S. L. Chuang, S. Schmitt-Rink, B. I. Greene, P. N. Saeta, and A. F. J. Levi, Phys. Rev. Lett. 68, 102 (1992).
[6] B. I. Greene, J. F. Federici, D. R. Dykaar, A. F. J. Levi, and L. Pfeiffer,Opt. Lett. 16, 48 (1991).
[7] D. M. Mittelman, S. Hunsche, L. Boivin, and M. C. Nuss, Opt. Lett. 22, 904 (1997).
[8] R. A. Cheville, R. W. McGowan, and D. Grischkowsky, OSA TOPS Vol. 13 Ultrafast Electronics and Optoelectronics, 222-227 (1997).